

1 **Pine and larch tracheids capture seasonal variations of climatic signal at moisture-limited sites**

2 Liliana V. Belokopytova¹, Elena A. Babushkina¹, Dina F. Zhirnova¹, Irina P. Panyushkina² & Eugene A. Vaganov^{1,3,4}


3 ¹Khakass Technical Institute, Siberian Federal University, 27 Shchetinkina St., Abakan, 655017, Russia

4 ²Laboratory of Tree-Ring Research, University of Arizona, 1215 W. Lowell St., Tucson, Arizona 85721, USA

5 ³Siberian Federal University, 79 Svobodny Pr., Krasnoyarsk, 660041, Russia

6 ⁴V. N. Sukachev Institute of Forest, SB RAS, 50/28 Akademgorodok, Krasnoyarsk, 660036, Russia

7 *Corresponding author:* Elena A. Babushkina. E-mail: babushkina70@mail.ru,

8 tel: +7-906-192-10-95,  <http://orcid.org/0000-0002-1355-4307>

9
10 **Key message:** Although the radial diameter and wall thickness of conifer tracheids from dry environments are
11 climatic-sensitive across the full ring area, each cell parameter has a specific zone in a ring where its climatic response
12 reaches the maximum.

13 **Abstract** Seasonal dynamics of the timing and rate in cell production and differentiation imprint climate signals
14 into intra-ring variations of anatomical wood structure (e.g. intra-annual density fluctuations). Despite recent
15 methodological advances in quantitative wood anatomy, our understanding of xylem response to climate at the finest scale
16 of intra-ring resolution is incomplete. The goal of this study is to investigate intra-ring changes of tracheid dimensions (cell
17 radial diameter and wall thickness) controlled by moisture stress. Anatomical wood parameters of *Pinus sylvestris* and
18 *Larix sibirica* from two drought-susceptible locations in Khakassia, South Siberia, were analysed. We found that inter-
19 annual variation of tracheid parameters regularly exceeds the variation between radial tracheid files. This suggests that the
20 climatic signal is recording throughout the entire ring. However, each cell parameter has a specific zone in the ring where
21 its climatic response reaches the maximum. The climatic response of the radial cell diameter has a temporal shift across the
22 ring, which is particularly apparent in pine rings. The climatic response of cell-wall thickness at the intra-ring scale has a
23 more complex pattern. Our results facilitate investigation of the climate impact on tree rings at the finest intra-ring scale by
24 quantifying the timing of climatic impact on ring structure and identifying specifically when climate impacts the formation
25 of a particular cell.

26 **Keywords** conifer trees; xylem; quantitative wood anatomy; tree-ring structure; climatic response; South Siberia

27 **Author contribution statement** EAV designed the study with input from EAB. DFZ supervised fieldwork and
28 measurements. LVB performed statistical analysis and prepared figures. All authors contributed to discussion of results and
29 writing the manuscript. LVB and IP wrote the English version of manuscript.

30 **Acknowledgements** This study was supported by the Russian Foundation for Basic Research (project no. 17-04-
31 00315). Collaborative activities of I. Panyushkina were sponsored by the CRDF-Global project #FSCX-18-63880-0. We

32 would like to thank Prof. S. W. Leavitt (University of Arizona) for proofreading of the manuscript. We are grateful to
33 editor and reviewers for their helpful comments.

34 **Conflict of interest** The authors declare that they have no conflict of interest.

35 **Introduction**

36 Annual tree rings are affected by environmental factors including climate. On the level of cell production, tree
37 rings record a climatic signal by means of changes in timing and rate of production (Prislan et al. 2013; Gričar et al. 2014;
38 Swidrak et al. 2014; Balducci et al. 2016). Changes in cell differentiation further translate into variations of xylem
39 anatomical structure (Yasue et al. 2000; Balducci et al. 2016; Ziaco and Biondi 2016). Quantitative wood anatomy can be
40 used to address research questions related to how climate changes the ring's cell structure, and how xylem anatomical
41 parameters could be utilized in climatic modelling (Panyushkina et al. 2003; Venegas-González et al. 2015; Singh et al.
42 2016; Castagneri et al. 2017; Wang et al. 2017). Recent advances in quantitative wood anatomy significantly improved the
43 efficiency and accuracy of xylem anatomical measurements (von Arx and Carrer 2014; Gärtner et al. 2015; von Arx et al.
44 2016; Prendin et al. 2017; Peters et al. 2018). New methodological tools available for analysis of xylem anatomical data
45 enable the employment of the wood structure parameters for climate reconstruction at very fine intra-seasonal scales well
46 beyond the conventional use of ring widths with annual or seasonal time resolution (Wheeler and Baas 1993; Wimmer et al.
47 2000; Panyushkina et al. 2003; Eilmann et al. 2009; Fonti et al. 2010). For example, earlywood measurements of vascular
48 parameters in ring-porous trees have been successfully used to evaluate the past moisture regime of the Mediterranean
49 region and the past temperatures of the temperate climates in Europe (Pérez-de-Lis et al. 2016; Puchałka et al. 2016;
50 García-González and Souto-Herrero 2017). It was also suggested that the intra-annual density fluctuations (IADFs) of tree
51 rings from arid environments appear to be a good indicator for short-term droughts during the growing season (Battipaglia
52 et al. 2010; Campelo et al. 2007; De Micco et al. 2012, 2016; Wilkinson et al. 2015; Zalloni et al. 2016). Analysis of the
53 radial cell diameter and cell wall thickness of conifer tracheids from moisture-stressed environments has shown a high
54 sensitivity of these parameters to moisture deficiency (Eilmann et al. 2009; Fonti and Babushkina 2016). Nevertheless, the
55 temporal resolution of the xylem climatic signals is not well understood.

56 Another important approach of quantitative wood anatomy research is modelling kinetics of seasonal ring growth
57 using estimates for the duration and rate of cell differentiation dynamics to theoretically validate parameters of tree-ring
58 anatomical structure (Dodd and Fox 1990; Deslauriers and Morin 2005; Rossi et al. 2006; Rathgeber et al. 2016; Castagneri
59 et al. 2017). The success of this approach results in the feedback scheme of climatic factors impacting wood anatomical
60 structure through the control of key processes of morphogenesis (Seo et al. 2008; Cuny et al. 2013, 2014; Rathgeber et al.
61 2016). Some research claims that only latewood cells have "climatic potential" (Cuny and Rathgeber 2016), although this
62 conclusion was drawn from small site studies. In contrast, other research indicates that climatic sensitivity of wood
63 structure in the form of IADF is observed not only in latewood but throughout the entire tree ring (Campelo et al. 2006;
64 Battipaglia et al. 2010, 2016; Babst et al. 2016). All these studies indicate that xylem anatomical parameters respond to

65 climate variations at the time of their formation, and furthermore xylem formation may be responding to climatic stress
66 with various strategies (Castagneri et al. 2017).

67 The main goal of this research was to evaluate the intra-ring dynamics of climatic signals in xylem anatomical
68 parameters of conifer trees growing in a moisture-stressed environment in order to understand the climatic sensitivity of
69 xylem at very fine intra-seasonal resolution. For this, we aim to 1) develop site chronologies of xylem anatomical
70 parameters and evaluate their statistical characteristics, 2) determine the relationship between tree-ring width, cell number
71 and mean cell size, 3) compare the intra-seasonal and inter-annual variability of xylem anatomical parameters, and
72 4) identify main climatic factors driving the anatomical ring structure. The study was conducted in the forest-steppe and
73 steppe zones of South Siberia where conifer tree growth is limited by both temperature and precipitation, and summer
74 droughts are often recorded. The forest stands comprise two dominant conifers, evergreen (Scots pine) and deciduous
75 (Siberian larch), to facilitate a comparison of xylem anatomical traits between two different tree species.

76 **Material and Methods**

77 *Site settings and climate*

78 The study area is situated on the margins of the Sayan-Altai Mountains in South Siberia. The landscape comprises
79 dry and cold depressions with steppes and forest-steppe ecotone, and mountain ranges covered predominantly with conifer
80 forests. The samples were collected from two sites in the Minusinsk depression (Fig. 1a). The Minusinsk site (MIN,
81 53°45'N, 91°56'E, 300 m a.s.l.) is located 15 km east of the Minusinsk weather station (#29866, 53°41'N, 91°40'E, 250 m
82 a.s.l.). The MIN site is covered with pine-birch forest on a chernozem soil layered with sand. The site is part of a large
83 isolated tree stand surrounded by dry grasslands of the steppe zone called the Minusinsk forest. The forest vegetation in this
84 dry environment is mainly sustained by extra moisture from numerous small lakes and rivers scattered throughout the area.
85 The Bidja site (BID, 54°00'N, 91°01'E, 660 m a.s.l.) is located in the forest-steppe zone of the Batenevsky Range foothills,
86 60 km northeast of the Minusinsk weather station. The trees were sampled in the pine-larch open canopy forest on grey
87 forest soils.

88 The climate of the study region is temperate extremely continental (Table S1; Alisov 1956). The annual average
89 air temperature varies from year to year in range from -1.5 to +4.1°C. Warmest temperatures occur from the end of June to
90 the first half of July, when daily values sometimes exceed 30°C. The annual sum of precipitation varies from 260 to 580
91 mm. About 90% of precipitation falls between April and October with a maximum in July. Vegetative season lasts
92 approximately from the third decade of April to the beginning of October, when daily temperatures are higher than 5°C.
93 However, onset of cambial activity can be delayed by moisture deficit in May in extremely dry years (cf. delay
94 observations in more arid conditions by Ren et al. 2015, 2018; Ziaco et al. 2018). Droughts may also occur later in the
95 season.

96 The foothills generally receive more precipitation (ca. 140 mm per year) and less warmth (ca. 0.7°C) than the
97 Minusinsk forest, which is hotter and dryer due to the elevational and latitudinal differences (Table S1). However, the
98 choice of sampling sites was aimed at reducing differences in soil moisture and microclimate conditions. We selected the
99 BID site on dry slope of the south-aspect with high insolation and rapid runoff of precipitation. At the same time, the MIN
100 site was selected on the flat landscape. Both sites have soils with below average humus content and water retention capacity
101 (Kolyago 1971). The assumption of relative similarity in local conditions between sites was further supported by
102 comparison of undercover vegetation (shrubs and herbs) at both sites, which comprised the same species and species with
103 similar water supply requirements.

104

105 *Tree-ring sampling and measurements*

106 The increment cores from Scots pine (*Pinus sylvestris* L.) at the MIN site and Siberian larch (*Larix sibirica* L.) at
107 the BID site were collected for this study. The wood surface preparation, tree-ring width (TRW) measurements and ring
108 crossdating were carried out according to standard procedures of dendrochronology (Stokes and Smiley 1968). Two site
109 TRW chronologies (indexed by detrending with negative exponential curves and then averaged; Cook, Kairiukstis, 1990)
110 were developed from 16 and 36 trees at the BID and MIN sites, respectively (Babushkina and Belokopytova 2014;
111 Belokopytova et al. 2018). For the anatomical measurement, we selected five trees from each site that have high correlation
112 with the site ring width chronology and were minimum 100-years old. Given the weak expression of the age trend in cell
113 parameters, such a restriction reduce the age impact on the study results (Vysotskaya and Vaganov 1989; Lei et al. 1996;
114 Eilmann et al. 2009).

115 After softening the cores by boiling in water, they were cut into thin sections (ca. 20- μ m thick) with a sledge
116 microtome (Microm HM 430; Thermo Fisher Scientific, USA) and then stained with an ethanol solution of 1% safranin. An
117 image of each micro-section was captured with an image system built from a digital camera connected to a microscope
118 (AXIOCam MRc5, Axio Imager D1; Zeiss, Germany, 400x magnification). Using captured images, we measured the
119 following radial parameters of tracheids in each tree ring: cell number (N), radial lumen diameter (LD) and double cell-wall
120 thickness. For this study we replicated the tracheid measurements along five cell radial files per a ring. The optimum
121 number of replications was determined by experimentation. Details are shown in the Electronic Supplementary Material
122 (ESM). Accuracy of measurements is ca. 0.01 μ m. The cell measurements were made for the interval 1965-2014 for MIN
123 pine and the interval 1976-2011 for BID larch. Measurements of cell dimensions were processed with Lineyka software
124 (Silkin 2010).

125 *Cell chronologies*

126 To distinguish cell dimensions developed during different phases of xylogenesis (Larson 1994), the measurements
127 were transformed into radial cell diameter ($CD = \text{lumen diameter} + \text{double cell wall thickness}$) and cell-wall thickness
128 (CWT) using the ProcessorKR software (Silkin 2010). Because the radial number of cells varies between rings and within a
129 ring, the cell diameter and wall thickness of each measured file were normalised to a constant number of cells per a ring
130 (Vaganov et al. 1985), which allows inter-annual and intra-ring comparison, and correlations between studied anatomical
131 parameters. In this case, we normalised the measurements to 15 cells (1...15). The ESM provides details on choice of this
132 cell number and procedure of normalisation. The individual tree series of cell diameter and wall thickness for each of the
133 fifteen normalised cells were averaged from the five replicated file measurements and then for the five sampled trees. A
134 total of 30 chronologies of tracheid anatomical parameters were developed for each site: 15 series for cell diameter and 15
135 series for wall thickness. Additionally, site cell number chronologies were built by averaging the number of cells per ring
136 from the five replicated file measurements of the five sampled trees. TRW series were calculated as the CD sum for a radial
137 cell file from a measured ring, and then used to crossdate cell chronologies. Crossdating was performed by comparison of
138 TRW series calculated from cells and measured directly from the same core. Also, mean cell diameter CD_{mean} was
139 calculated for each ring, and its time series for individual trees were investigated.

140 For inter-chronology comparison, the site cell chronologies were transformed into Z-scores (standardised to mean
141 value of 0 and standard deviation of 1). Consequently, we analysed a dataset of 64 site chronologies: 15 CD, 15 CWT,
142 TRW series, and N chronologies each for both pine and larch. The length of the cell chronologies is 50 years (1965-2014)
143 for pine and 36 years (1976-2011) for larch parameters.

144 *Statistical analysis*

145 Key properties of variation in the cell parameters were described with arithmetic mean, standard deviation, and
146 coefficient of variation, which is a ratio of standard deviation to arithmetic mean (Fritts 1976; Wigley et al. 1984). The
147 variation of tracheid anatomical parameters was studied at various scales: inter-annual, intra-ring and inter-files, and
148 visualized with time series (cell chronologies) and tracheidograms. A tracheidogram is a plot of intra-ring variation of an
149 anatomical parameter in the radial direction according to the relative cell position within the ring as calculated for the 15
150 normalised cells per ring in this case (Panyushkina et al. 2003; Vaganov et al. 2006). The tracheidograms were also used to
151 derive patterns of ring division in the earlywood, transition wood, and latewood. Latewood was defined on the basis of
152 Mork's empirical criterion of $CWT > 0.25 \text{ LD}$ (Denne, 1989). For the transition wood threshold was defined with $CWT >$
153 0.10 LD , which coincides with the onset of statistically significant increase of CWT.

154 Pearson correlation coefficients and simple linear regression models were calculated for evaluation of
155 relationships between various cell parameters and their response to climate. In this study, daily observation data of mean

156 temperature (T) and precipitation (P) for May–September season from the Minusinsk weather station for the interval 1964
157 to 2011 were used. In addition to the observations, we calculated two moisture regime monthly indices from T and P series
158 of the Minusinsk station. Selyaninov hydrothermal coefficient (HTC) is calculated with the formula $HTC = 10 \cdot \sum P / \sum T$
159 (Selyaninov 1937). The wetness index (WI) was adopted from Lei et al. (2014) and the equation was modified as $WI =$
160 $10 \cdot \sum \log(P + 1) / \sum T$ to take into account the possibility of zero P). To investigate climate–growth relationships we used
161 May–September daily temperature series averaged over a 20-day window with 1-day moving step, and precipitation series
162 summed over the same window and step (Fig. 1b). This statistical approach has been recently used in analysis of ring
163 cambial dynamics and cell parameters (e.g. Carrer et al. 2017; Castagneri et al. 2017). The climate correlation analysis was
164 performed for chronologies of tree-ring width, cell number, and cell diameter and cell wall thickness for each normalised
165 cell.

166 Additionally, pointer years were used to compare the wood anatomical structure formed under pluvial and drought
167 conditions. This analysis was only performed for pine that has a longer interval of tracheid measurements than larch, and a
168 sufficient number of pointer years. The pointer years were defined in the tree-ring width site chronology, where a TRW
169 exceeding the mean plus 1σ indicates a positive pointer year and TRW less than the mean minus 1σ indicates a negative
170 one.

171 **Results**

172 *Mean of cell measurements and tree-ring width*

173 Tree-ring width parameters strongly relate to the number of cells. Coefficients of determination for linear
174 regressions between these two parameters are above 0.9 for individual trees of pine and larch, and ca. 0.89 for the averaged
175 site series, with all relationships significant at $P \leq 0.0001$ (Fig. 2, Table 1). Since these two parameters are nearly
176 proportional (intercept of the regression line is close to zero), the slope of linear regression can be considered to be an
177 estimation of the mean radial cell diameter of individual trees CD_{mean} . Linear regression estimation of the mean cell
178 diameter is ca. 3–4 μm higher than its directly calculated value (average value from all measured rings for individual tree).
179 The individual tree series of mean cell diameters exhibit no statistically significant long-term age-related trends for either
180 species ($P > 0.1$ for linear approximations of trends). The average number of cells per ring and the mean cell diameter are
181 statistically independent regardless of the calculation method.

182 *Variation of cell anatomical parameters*

183 Analysis of replicated measurements indicates a small range of CD and CWT residual inter-file variations after
184 averaging over five files. Coefficient of variation is on the average 4–5% and never exceeds 10%, without regularities
185 within a ring (dotted line in Fig. 3). In contrast, the inter-annual variations of the cell anatomical parameters are much
186 higher. In the earlywood zone defined by the first seven normalised cells for pine and first four normalised cells for larch,

187 the CD and CWT size inter-annual variation is practically constant. In the transition zone (normalised cell positions 8...10
188 for pine and 5...8 for larch) it abruptly increases. In the latewood zone (normalised cell positions 11...15 for pine and
189 9...15 for larch) the inter-annual variation gradually declines (solid and dashed lines in Fig. 3). The inter-annual variation
190 for CD changes throughout the ring with a smaller range than for CWT: maximum coefficients of variation for CD is 24%
191 for pine and 43% for larch, and for CWT 33% and 54%, respectively. The main difference between species is relative
192 width of different zones within the ring, with much wider latewood for larch. The CWT of earlywood is less variable in
193 larch than in pine. This intra-ring pattern is consistent in our data. However, some fluctuations in the CD and CTW
194 variations were observed between individual trees (Table S2). We noticed that trees with a larger mean cell diameter have a
195 higher inter-annual variation of the earlywood CD. Trees with larger cell production (higher N) have a higher inter-annual
196 variation of the latewood CD and CWT. Generally, the variation of site cell chronologies is considerably less than of their
197 individual series. Additionally, the variation of site tree-ring width indexed chronologies is 20.6% for pine and 36.3% for
198 larch, which is much higher than for cell parameters' site chronologies (Table S3).

199 *Common variance in cell chronologies*

200 Figure 4 shows some of cell site chronologies and respective series of individual trees. The common component of
201 variance in cell chronologies varies between cell parameters and ring zone. CD has the highest correlation between
202 individual tree series in the transition wood (normalised cell positions 7...8 for pine and 4...5 for larch), whereas the lowest
203 correlations are in the latewood (Table S4). The CWT correlation pattern is the opposite, with maximum in the middle of
204 latewood (normalised cell number 13 for pine and 11-12 for larch), and the lowest correlations in the earlywood.
205 Correlations of individual tree series and site chronologies are generally higher for the CD parameter.

206 Correlation between cell site chronologies of different normalised cell positions depends on the ring zone (Table
207 S5, S6). The correlation coefficients between the cell chronologies have the maximum values between adjacent positions
208 (reaching 0.94 for CD and 0.97 for CWT). Interestingly, most correlations between the cell parameters of earlywood and
209 latewood are not significant. For both tree species, close correlations between the CWT chronologies extend to a greater
210 distance within the boundaries of earlywood and latewood ring zones. CD, on the contrary, shows the highest correlations
211 and greatest distances between significantly correlated cell chronologies in the transition zone. The inter-ring pattern
212 matches for the studied tree species.

213 *Correlation of chronologies with climatic factors*

214 Tree-ring width (and cell number) has a complex response to climate, which is similar for both tree species: high
215 temperature of the first half of growing season suppresses growth but amount of precipitation shows a positive effect (Fig.
216 5, Fig. S2). The negative impact of temperature reaches the maximum in late May and early July, then in mid-August. The

217 periods of growth stimulated by moisture influx are almost the same: May to early June and first half of July. The response
218 of tree-ring parameters to moisture indices HTC and WI differs very little from the precipitation response.

219 For pine, the CD response to climate shows a gradual change across the ring. Maximum correlations shift: they are
220 observed from May to mid-June for first cells, in mid-July for the transition wood chronologies, and in the end of August
221 for the latewood. The effect of precipitation on CD is more pronounced for the earlywood and transition wood. It should
222 also be noted that the duration of the climatic response decreases in the last cells. CWT responds to the positive effect of
223 precipitation between mid-July and mid-August. This relationship is significant only for the transition wood cells and the
224 first few cells of latewood (cell positions 8...12). The negative effect of temperatures has a longer seasonal window
225 ranging from July to August for the entire ring. We observed an inversion of the climate effect on CWT in June when dry
226 and warm weather led to the formation of thicker cell walls throughout the ring. The maximum strength of this signal is
227 recorded at cell positions 8...12. Furthermore, CWT is negatively correlated with both climatic parameters during the
228 second half of August and the beginning of September.

229 For larch, CD and CWT responses are similar to the pine anatomical parameters but the climatic signal is weaker.
230 The positive impact of precipitation and negative impact of temperature on larch CD occur from May to early June in the
231 beginning of earlywood and from late June to early July in the last cells of latewood. The climatic inversion can still be
232 seen in the CWT series but with a much smaller magnitude. The precipitation impact is positive from mid-June to mid-July.
233 The climatic signals of anatomical parameters for both studied tree species correspond to timing of corresponding phases of
234 cell differentiation.

235 Pointer-year analysis for pine identified five negative (1964, 1965, 1974, 1998, 2012) and five positive (1970,
236 1971, 1982, 1995, 2007) pointer years. Figure 6 shows variations of climatic and anatomical parameters during these two
237 sets of pointer years. Precipitation during the positive pointer years is up to 5 times more from May to the first half of June
238 than in the negative pointer years, and up to 2.5 times more during the interval of July to first half of August. Temperatures,
239 on the other hand, are significantly higher for the negative pointer years during the same periods (up to 3.7°C and up to
240 2.6°C, respectively). However, there is no significant difference between positive and negative pointer years at $P<0.05$ in
241 the second half of June. Tracheidograms of the pointer years show that the tracheids are larger in the wet years than in the
242 dry ones. The tracheids of the earlywood and latewood have significantly larger cell diameters: difference is 4-7 μm or 11-
243 17% at cell positions 1...8, and 3-7 μm or 13-41% at positions 12...15, whereas the transition wood CD shows no
244 significant difference between the positive and negative pointer years. The CWT is significantly larger (at $P<0.05$) during
245 positive years for cell positions 10...15 with maximum difference ca. 1.2 μm or 31% at positions 12.

246 **Discussion**

247 *Relationships between cell parameters and cell production*

248 Variance of wood anatomical parameters contains information independent of cell production and radial growth
249 (Wimmer 2002; Rossi et al. 2012). Strong linear dependence of TRW on the cell number indicates that the average size of
250 tracheids is stable during the observation period. The CD_{mean} does not have significant time dependency on age and size of
251 individual trees or on climatic change. Age- and size-related decreasing rate and duration of cambial activity (leading to
252 long-term trends in TRW and cell number) can last for centuries (Rossi et al., 2008; Li et al. 2013). However, for cell
253 anatomical parameters and wood density as their derivative, there is evidence of such trends present predominantly during
254 the first decades of tree lifespan (e.g. Pritzkov et al. 2014; Pacheco et al. 2016; see also theoretical reasoning by hydraulic
255 requirements in Carrer et al. 2015). This means that we can observe age trends in wood anatomy only when the pith wood is
256 included in anatomical measurements (cf. Ziaco et al. 2016). Therefore in our study, absence of age trend in anatomical
257 parameters is most certainly due to exclusion of the earliest 50 years (or more) of tree growth. The averaging of series
258 between trees within one site slightly weakens the relationship between radial tree growth and cell production. Previous
259 research found that the linear regression slope between TRW and N in larch trees in the study region varies depending on
260 site habitat conditions (Babushkina 2011). Our results suggest the average size of tracheids depends on a combination of
261 habitat (at site and individual tree scale) and tree genetics (Fonti et al. 2010).

262 A number of studies have shown that the relationship between tracheid size and cell production in all ring zones is
263 described with an inverted negative exponential curve for narrow rings and horizontal straight line for wide rings (Vaganov
264 et al. 1985; Babushkina 2011). The same relationship should be true for the mean cell diameter, but only a small share of
265 rings are narrow enough to observe the dependence of cell size on the cell number (Fig. S3). It is possible that the lack of
266 the relationship between the mean cell diameter and mean cell number is explained by relatively mild climatic conditions in
267 the study area. CWT depends even less on cell production and shows a weak relationship with CN and TRW, since the wall
268 maturation occurs later in the growing season.

269 *Variation of anatomical parameters*

270 Xylem anatomy records information about the climate impact on various scales: intra-ring and inter-annual. Intra-
271 ring variations determine the ring structure, which includes earlywood (large-diameter thin-walled tracheids), transition
272 wood, and latewood (small-diameter thick-walled tracheids). The procedure of normalising the measured radial cell files to
273 a constant cell number divides a ring into narrow zones, and this ring partitioning isolates the variance pattern of
274 anatomical parameters of each ring zone, and ascribes the climatic signal to these ring zones (Panyushkina et al. 2003;
275 Deslauriers et al. 2003a; Vaganov et al. 2006; Olano et al. 2012). Another source of variance in the anatomical

276 measurements arises from the position of tracheid across the circumference of the ring, i.e. tracheids from different radial
277 files. Averaging xylem measurements over several cell files significantly reduces this type of variance (Seo et al. 2014).

278 Inter-annual variation of anatomical parameters is the main focus of dendroclimatic studies that use this fine
279 temporal scale of year-to-year variance for modelling of retrospective variability of climate. Inter-annual variations of the
280 average of five files of CD and CWT are higher than the inter-file variance. Our study suggests that the intra-annual
281 variance is constrained by extrinsic factors (e.g. temperature and precipitation). The pattern of inter-annual variation
282 changes across a ring, which makes it possible to track the inter-annual climatic signal between the ring zones. Cells of
283 earlywood have a persistent intra-ring range in the CD and CWT within earlywood: CD has the maximum and CWT has
284 the minimum for a given tree species at particular habitat. This specific property of earlywood cell variance also persists at
285 the inter-annual time scale.

286 Additionally, the ratio between the earlywood and latewood also varies significantly from year-to-year, which
287 leads to inter-annual offset in the position of the transition wood zone of the normalised tracheidogram. The switch of cells
288 in the middle of tracheidogram between the earlywood and latewood introduces additional variance and results in an
289 increased annual variability of cell parameters in transition zone. The seasonal processes involving nutrient accumulation
290 are contingent on environmental settings, so they should also influence xylogenesis (Cuny et al. 2016). It is known that the
291 formation of the secondary wall requires substantially more resources than the expansion of the primary wall (Hall et al.
292 2013; Overdieck 2016). This may explain the higher variation of CWT as compared to CD in the transition wood and
293 especially latewood, and the stronger relationship of these cell series with climatic conditions. The duration of cell
294 expansion decreases from the earlywood to latewood, whereas the duration of secondary wall deposition increases (Cuny et
295 al. 2013, 2014; Rossi et al. 2006; Rathgeber 2017). This longer exposure of latewood cell wall deposition to climate
296 influence induces a greater variation of the corresponding cell parameter. The variation of anatomical parameters of the last
297 few cells decreases synchronously, since the secondary wall deposition is limited by the small size of the tracheids (CWT
298 cannot exceed 0.5 of CD).

299 *Inter-species differences*

300 Our results suggest two studied conifer tree species have common patterns of variance of the anatomical
301 parameters. The only visible difference between pine and larch xylem is seen in a greater proportion of latewood for larch.
302 Similar ring structure is observed in oak, which is a well-studied ring-porous deciduous tree species (Büyüksarı et al.
303 2017). Large vessels developed at the very beginning of the growing season support the intensive emergence and growth of
304 foliage. A wide zone of small vessels in the latewood determines the high density of oak wood. Something similar can be
305 assumed for larch, which is also a deciduous species. We note that the radial diameter of cells (and consequently the lumen
306 size) in larch earlywood is significantly larger than that of pine (Fig. 3). This phenomenon shifts the functional

307 characteristics of larch ring structure closer to oak as well. The deployment of new needles for larch at the onset of the
308 growing season is also coordinated with formation of large tracheids in the earlywood through the auxin synthesis in buds
309 breaking en masse. Later, end of primary growth regulates a xylogenesis switch toward smaller tracheids with thicker
310 walls. In turn, this switch requires a significant influx of nutrients into the xylem (Funada et al. 2001; Singh et al. 2012). On
311 the other hand, climatic and soil-landscape conditions are not identical at both sites. This fact further reinforces differences
312 in tree growth and its climatic response. For example, less significant climatic response of larch can be related to slightly
313 cooler and wetter growth conditions. To distinguish functional species-specific differences and impact of local growth
314 conditions with more certainty, further research is required.

315 *Common variance of cell parameters*

316 Our study showed distinctive partitioning of the common variance related to climate in the cell parameter
317 chronologies. Firstly, the highest correlation between individual tree series occurs in the ring zone with the maximum size
318 of anatomical parameters (Table S4). It suggests that the strength of cell parameter' common variance including response to
319 climate depends on the duration and rate (intensity) of the corresponding phase of tracheid differentiation, because these
320 kinetic characteristics contribute to the final size of cell parameters (see Anfodillo et al. 2012; Cuny 2013; Cuny et al. 2013,
321 2014). Secondly, the shift of high correlations toward the transition wood is an indicator for synchronous fluctuation of the
322 earlywood/latewood ratio at the site. It is driven by synchronized extrinsic factors (e.g. temperature, day length) that trigger
323 the switch of cell formation from earlywood to latewood (Begum et al. 2016; Petterle et al. 2013), and climatically-induced
324 variance in cell production before and after this switch.

325 Intrinsic factors (genetics) impart stable wood structure and lessen common variance of the earlywood CWT series
326 (Darikova et al. 2013). This assumption is also supported by other studies, e.g. low common variance in the mean CWT
327 series observed in tree-rings with predominant earlywood (Ziaco et al. 2016). This can explain the analogous dynamics of
328 CWT in adjacent cell positions of the earlywood, which is especially evident for pine characterised by a relatively large
329 proportion of earlywood in the ring (Table S6). The periods of tracheid differentiation partially overlap in close and
330 especially adjacent tracheid positions; it means that common signals of CWT or CD chronologies overlap for close cell
331 positions. This overlapping leads to the observed pattern of correlations between cell parameter series of different
332 normalised cell positions (Table S5, S6, also see similar patterns in Panyushkina et al. 2003; Castagneri et al. 2017), i.e., as
333 the distance between cell positions increases, the correlations decrease rapidly from very high values to insignificant ones.

334 *Climate–growth relationships*

335 Climatic impact on the radial growth of conifer trees is common in semi-arid regions. Moisture from precipitation
336 stimulates tree growth, while high temperature promotes evapotranspiration and creates water stress. TRW integrates this
337 impact mainly during cambial activity through the rate of cell production. We note that relatively high precipitation

338 observed in late June and late July (Fig. 1b) significantly weakens the TRW climatic signal during this period (Fig. 5). This
339 response is explained by the limiting role of both temperature and precipitation on the soil moisture and hydrological
340 regime. This is also true for the response of chronologies to other climatic parameters related to humidity. Less pronounced
341 climate response of larch TRW compared with pine TRW corresponds to the patterns of xylem climatic response. A short
342 lag at the beginning of larch climate response observed in TRW and cell chronologies may be due to combination of later
343 onset of growing season at the BID site and the necessity of development of assimilation apparatus (needles). Kraus et al.
344 (2016) described a similar temporal pattern with the same time of bud burst and onset of cambial activity for evergreen
345 spruce and a three-week delay of secondary growth for deciduous beech.

346 The climate impact on CD shows a similar pattern, but the period of high impact shifts across the ring as new cells
347 form (Fig. 5). Radial cell diameter is linked to weather conditions during the process of cell expansion (Deslauriers et al.
348 2003b; Vaganov et al. 2011). Additionally, the time interval with significant correlation of climate and CD can be partially
349 amplified by the procedure of cell number normalisation, which bears more on the xylogenesis process than the calendar
350 dates (Vaganov et al. 2006). Many previous studies noted that wood formation, including the cell division and
351 differentiation, may start and end at different calendar dates in different years (Prislan et al. 2013; Gričar et al. 2014;
352 Swidrak et al. 2014; Ziaco and Biondi 2016; Yang et al. 2017). In more arid areas, the timing of tree-ring development
353 closely depends on both temperatures and precipitation, which was observed on the northeastern Tibetan Plateau and
354 especially in the Mojave Desert mountains (Ren et al. 2015, 2018; Ziaco et al. 2018). A similar pattern can also be expected
355 in the Minusinsk depression, as supported by simulation and seasonal observations of xylogenesis (Popkova et al. 2015,
356 2018). Therefore, we cannot exclude the influence of climate impact on the final radial diameters during the period when
357 the cells are still situated within the cambial zone (Vaganov et al. 2006; Cuny et al. 2014).

358 Some anatomical parameters may have weak climatic response and low inter-annual variation in comparison to
359 cell production and total ring growth. Cell number and TRW integrate the effect of climatic fluctuations over a much longer
360 interval compared to anatomical parameters of individual cells, which results in higher values of annual variations. The
361 effect of extrinsic factors on the process of cell division, duration and rate (the number of cells produced per time unit)
362 changes in one direction (Rossi et al. 2014). This leads to nonlinear relationship of this effect with the cell production. As
363 shown by Balducci et al. (2016), the kinetics of later cell differentiation processes has a built-in compensatory mechanism:
364 suppression of the expansion rate of an individual cell or deposition of a secondary wall under the stressed conditions is
365 partially compensated with increasing time for this cell residing in the corresponding zone of cell differentiation. Thus, the
366 climate effect on the anatomical structure of the ring will be somewhat dampened. This phenomenon is possibly driven by
367 the genetic mechanism of successive phases in tracheid differentiation that begins with division and ends with programmed
368 cell death. This was confirmed by Darikova et al. (2013) for Scots pine and Siberian pine with genetically determined inter-

369 species difference in cell growth that was monitored on a single plant (graft and rootstock), i.e. under uniform external
370 conditions and hormone concentrations. Cuny et al. (2014) showed the intrinsic compensation mechanism with negative
371 relationship between the rate and duration of cell differentiation processes.

372 The inversion of CWT climate response in June indicates that moisture deficit may prompt developing not only
373 smaller but also thicker-walled cells. As a result, the cell's water-conducting capacity and subsequently transpiration
374 decrease as a part of compensating mechanism for adapting trees to water stress (Nicholls and Waring 1977; Hacke and
375 Sperry 2001; Sterck et al. 2008). CWT of the last tracheids in the latewood is limited by CD, which leads to their similar
376 reaction to temperature.

377 The combination of climate responses for both anatomical parameters yields cumulative response of wood density
378 to the moisture fluctuations. Unlike many other regions where maximum density is a proxy for temperatures, often having
379 stronger climatic signal than TRW (Sun et al. 2016; Rathgeber 2017; Stine and Huybers 2017), in the studied region the
380 ring wood density has a good potential for being a moisture proxy.

381 Our comparison of the ring xylem structure formed during the driest and wettest years (pointer years) suggests that
382 even drastic differences in moisture availability are only moderately recorded in the studied anatomical parameters. This
383 once again confirms the manifestation of a compensatory mechanism in the kinetics of cell differentiation. It is interesting
384 that there is a zone of no significant differences between driest and wettest years in tracheidograms of both cell parameters,
385 which for CWT occur in earlier cell positions than for CD. As for the seasonal climate, the second half of June appears to
386 be the interval with minor differences in climate between pointer years. This points to the temporal shift in climatic effects
387 on wood formation due to timing of cell differentiation at the intra-ring scale as discussed earlier.

388 **Conclusion**

389 The robust linear relationship between TRW and cell production contains no age-related changes, but varies
390 between individual trees. The estimated variations in the cell parameters suggest the sensitivity of the wood structure to
391 fluctuation of extrinsic conditions, albeit uneven, distributes throughout the entire ring. In contrast to the mean ring
392 characteristics like TRW, the timing of environmental impacts is individual for each cell in accordance with the spatial-
393 temporal organisation of the cell production and cell differentiation processes. In addition to the higher temporal resolution
394 of the climate response, the cell parameters are less variable, which is associated with the genetically determined structure
395 of tree rings and the compensatory mechanism in the kinetics of cell development.

396 The xylem anatomical parameters can provide valuable information on the retrospective variability of
397 precipitation and temperature at very fine seasonal resolution. Although the radial diameter and wall thickness of conifer
398 tracheids from dry environments are climatic-sensitive across the complete ring area, each cell parameter has a specific

399 zone in a ring where its climatic response reaches the maximum or the minimum. This study indicates good potential for
400 employing maximum wood density as a proxy of moisture regime in the semi-arid regions of South Siberia.

401 The results of this research open up new possibilities for studying the impact of climatic factors on the tree growth
402 with very fine temporal resolution. Therefore, with respect to possible future research, it would be interesting to compare
403 the seasonal kinetics of cell differentiation and the xylem anatomy–climate relationships to refine the theoretical algorithms
404 of tree growth models.

405

406 **References**

- 407 Alisov BP (1956). Climate of the USSR. Moscow State University, Moscow (**In Russian**)
- 408 Anfodillo T, Deslauriers A, Menardi R, Tedoldi L, Petit G, Rossi S (2012) Widening of xylem conduits in a
409 conifer tree depends on the longer time of cell expansion downwards along the stem. J Exp Bot 63:837-845. doi:
410 10.1093/jxb/err309
- 411 von Arx G, Carrer M (2014). ROXAS – A new tool to build centuries-long tracheid-lumen chronologies in
412 conifers. Dendrochronologia 32(3):290–293. doi: 10.1016/j.dendro.2013.12.001
- 413 von Arx G, Crivellaro A, Prendin AL, Čufar K, Carrer M (2016) Quantitative wood anatomy – practical
414 guidelines. Front plant sci 7:781. doi: 10.3389/fpls.2016.00781
- 415 Babst F, Wright WE, Szejner P, Wells L, Belmecheri S, Monson RK (2016). Blue intensity parameters derived
416 from Ponderosa pine tree rings characterize intra-annual density fluctuations and reveal seasonally divergent water
417 limitations. Trees 30(4):1403–1415. doi: 10.1007/s00468-016-1377-6
- 418 Babushkina EA (2011) Influence of climatic factors and growing conditions on the variability of radial growth and
419 the structure of tree rings. Dissertation, Siberian Federal University, Institute of Forest SB RAS, Krasnoyarsk (**In Russian**)
- 420 Babushkina EA, Belokopytova LV (2014) Climatic signal in radial increment of conifers in forest steppe of
421 Southern Siberia and its dependence on local growing conditions. Russ J Ecol 45(5):325–332. doi:
422 10.1134/S1067413614050038
- 423 Babushkina EA, Belokopytova LV, Kostyakova TV, Kokova VI (2018) Earlywood and latewood features of *Pinus*
424 *sylvestris* in semiarid natural zones of South Siberia. Russ J Ecol. 49(3): 209-217. doi: 10.1134/S1067413618030013
- 425 Balducci L, Cuny HE, Rathgeber CB, Deslauriers A, Giovannelli A, Rossi S (2016) Compensatory mechanisms
426 mitigate the effect of warming and drought on wood formation. Plant Cell Environ 39(6):1338–1352. doi:
427 10.1111/pce.12689
- 428 Battipaglia G, De Micco V, Brand WA, Linke P, Aronne G, Saurer M, Cherubini P (2010) Variations of vessel
429 diameter and $\delta^{13}\text{C}$ in false rings of *Arbutus unedo* L. reflect different environmental conditions. New Phytol 188(4): 1099–
430 1112. doi: 10.1111/j.1469-8137.2010.03443.x
- 431 Battipaglia G, Campelo F, Vieira J, Grabner M, De Micco V, Nabais C et al (2016) Structure and function of
432 intra-annual density fluctuations: mind the gaps. Front Plant Sci 7:595. doi: 10.3389/fpls.2016.00595
- 433 Belokopytova LV, Babushkina EA, Zhirnova DF, Panyushkina IP, Vaganov EA (2018) Climatic response of
434 conifer radial growth in forest-steppes of South Siberia: comparison of three approaches. Contemp Probl Ecol 11(4): 366–
435 376 doi: 0.1134/S1995425518040030

436 Begum S, Kudo K, Matsuoka Y, Nakaba S, Yamagishi Y, Nabeshima E et al (2015) Localized cooling of stems
437 induces latewood formation and cambial dormancy during seasons of active cambium in conifers. *Ann Bot* 117(3):465–
438 477. doi: 10.1093/aob/mcv181

439 Büyüksarı Ü, As N, Dündar T (2017) Intra-ring properties of earlywood and latewood sections of sessile oak
440 (*Quercus petraea*) wood. *BioResour* 13(1):836–845.

441 Campelo F, Nabais C, Freitas H, Gutiérrez E (2006) Climatic significance of tree-ring width and intra-annual
442 density fluctuations in *Pinus pinea* from a dry Mediterranean area in Portugal. *Ann For Sci* 64(2):229–238. doi:
443 10.1051/forest:2006107

444 Carrer M, von Arx G, Castagneri D, Petit G (2015). Distilling allometric and environmental information from time
445 series of conduit size: the standardization issue and its relationship to tree hydraulic architecture. *Tree Physiol* 35(1):27–33.
446 doi: 10.1093/treephys/tpu108

447 Carrer M, Castagneri D, Prendin AL, Petit G, von Arx G (2017) Retrospective analysis of wood anatomical traits
448 reveals a recent extension in tree cambial activity in two high-elevation conifers. *Front Plant Sci* 8:737. doi:
449 10.3389/fpls.2017.00737

450 Castagneri D, Fonti P, von Arx G, Carrer M (2017) How does climate influence xylem morphogenesis over the
451 growing season? Insights from long-term intra-ring anatomy in *Picea abies*. *Ann Bot* 119(6):1011–1020. doi:
452 10.1093/aob/mcw274

453 Cook ER, Kairiukstis LA (eds.) (1990) *Methods of Dendrochronology. Application in Environmental Sciences.*
454 Kluwer Acad. Publ., Dordrecht; Boston; London.

455 Cuny H (2013) Dynamique intra-annuelle de la formation du bois de trois espèces de conifères (sapin pectiné,
456 épicéa commun, pin sylvestre) dans les Vosges. PhD thesis. Université de Lorraine, Nancy (**In French**)

457 Cuny HE, Rathgeber CB, Kiessé TS, Hartmann FP, Barbeito I, Fournier M (2013) Generalized additive models
458 reveal the intrinsic complexity of wood formation dynamics. *J Exp Bot* 64(7):1983–1994. doi: 10.1093/jxb/ert057

459 Cuny HE, Rathgeber CB, Frank D, Fonti P, Fournier M (2014) Kinetics of tracheid development explain conifer
460 tree-ring structure. *New Phytol* 203(4):1231–1241. doi: 10.1111/nph.12871

461 Cuny H, Rathgeber C (2016) Xylogenesis: Coniferous trees of temperate forests are listening to the climate tale
462 during the growing season, but only remember the last words! *Plant Physiol* 171:306–317. doi: 10.1104/pp.16.00037

463 Darikova YA, Vaganov EA, Kuznetsova GV, Grachev AM (2013) Changes in the anatomical structure of tree
464 rings of the rootstock and scion in the heterografts of Siberian pine. *Trees* 27(6):1621–1631. doi: 10.1007/s00468-013-
465 0909-6

466 De Micco V, Battipaglia G, Brand WA, Linke P, Saurer M, Aronne G, Cherubini P (2012) Discrete versus
467 continuous analysis of anatomical and $\delta^{13}\text{C}$ variability in tree rings with intra-annual density fluctuations. *Trees* 26(2):513–
468 524. doi: 10.1007/s00468-011-0612-4

469 De Micco V, Battipaglia G, Balzano A, Cherubini P, Aronne G (2016) Are wood fibres as sensitive to
470 environmental conditions as vessels in tree rings with intra-annual density fluctuations (IADFs) in Mediterranean species?
471 *Trees* 30(3):971–983. doi: 10.1007/s00468-015-1338-5

472 Denne M (1989) Definition of latewood according to Mork. *Iawa Bull* 10:59–62. doi: 10.1163/22941932-
473 90001112.

474 Deslauriers A, Morin H, Begin Y (2003a) Cellular phenology of annual ring formation of *Abies balsamea* in the
475 Quebec boreal forest (Canada). *Can J For Res* 33(2), 190–200. doi: 10.1139/x02-178

476 Deslauriers A, Morin H, Urbinati C, Carrer M (2003b) Daily weather response of balsam fir (*Abies balsamea* (L.)
477 Mill.) stem radius increment from dendrometer analysis in the boreal forests of Quebec (Canada). *Trees* 17:477–484. doi:
478 10.1007/s00468-003-0260-4

479 Deslauriers A, Morin H (2005) Intra-annual tracheid production in balsam fir stems and the effect of
480 meteorological variables. *Trees* 19(4):402–408. doi: 10.1007/s00468-004-0398-8

481 Dodd RS, Fox P (1990) Kinetics of tracheid differentiation in Douglas-fir. *Ann Bot* 65(6):649–657. doi:
482 10.1093/oxfordjournals.aob.a087983

483 Eilmann B, Zweifel R, Buchmann N, Fonti P, Rigling A (2009) Drought-induced adaptation of the xylem in Scots
484 pine and pubescent oak. *Tree Phys* 29(8):1011–1020. doi: 10.1093/treephys/tpp035

485 Fonti P, von Arx G, García-González I, Eilmann B, Sass-Klaassen U, Gärtner H, Eckstein D (2010) Studying
486 global change through investigation of the plastic responses of xylem anatomy in tree rings. *New Phytol* 185(1):42–53. doi:
487 10.1111/j.1469-8137.2009.03030.x

488 Fonti P, Babushkina EA (2016) Tracheid anatomical responses to climate in a forest-steppe in Southern Siberia.
489 *Dendrochronologia* 39:32–41. doi: 10.1016/j.dendro.2015.09.002

490 Fritts HC (1976) *Tree rings and climate*. Academic Press, London, New York, San Francisco.

491 Funada R, Kubo T, Tabuchi M, Sugiyama T, Fushitani M (2001) Seasonal variations in endogenous indole-3-
492 acetic acid and abscisic acid in the cambial region of *Pinus densiflora* Sieb. et Zucc. stems in relation to earlywood-
493 latewood transition and cessation of tracheid production. *Holzforschung* 55(2):128–134. doi: 10.1515/HF.2001.021

494 García-González I, Souto-Herrero M (2017) Earlywood vessel area of *Quercus pyrenaica* Willd. is a powerful
495 indicator of soil water excess at growth resumption. *Eur J For Res* 136(2):329–344. doi: 10.1007/s10342-017-1035-6

496 Gärtner H, Cherubini P, Fonti P, von Arx G, Schneider L, Nievergelt D et al (2015) A technical perspective in
497 modern tree-ring research-how to overcome dendroecological and wood anatomical challenges. *J Vis Exp* 97:e52337. doi:
498 10.3791/52337

499 Gričar J, Prislan P, Gryc V, Vavrčik H, de Luis M, Čufar K (2014) Plastic and locally adapted phenology in
500 cambial seasonality and production of xylem and phloem cells in *Picea abies* from temperate environments. *Tree Physiol*
501 34(8):869–881. doi: 10.1093/treephys/tpu026

502 Hacke UG, Sperry JS (2001) Functional and ecological xylem anatomy. *Perspect Plant Ecol, Evol Syst* 4:97–115.
503 doi: 10.1078/1433-8319-00017

504 Hall M, Medlyn BE, Abramowitz G, Franklin O, Råntfors M, Linder S, Wallin G (2013) Which are the most
505 important parameters for modelling carbon assimilation in boreal Norway spruce under elevated [CO₂] and temperature
506 conditions? *Tree Physiol* 33(11):1156–1176. doi: 10.1093/treephys/tpt014

507 Kolyago VA (1971) Soils of the forest-steppe and steppe of the Minusinsk depression and their agrochemical
508 characteristics. In: Sokolov AV, Orlovsky NV (eds.) *Agrochemical characteristics of the USSR soils. Middle Siberia*. pp.
509 131-181. Nauka, Moskow (**In Russian**)

510 Kraus C, Zang C, Menzel A (2016) Elevational response in leaf and xylem phenology reveals different
511 prolongation of growing period of common beech and Norway spruce under warming conditions in the Bavarian Alps. *Eur*
512 *J For Res* 135(6):1011–1023. doi: 10.1007/s10342-016-0990-7

513 Larson PR. (1994) *The vascular cambium. Development and structure*. Springer-Verlag, Berlin.

514 Lei H, Milota MR, Gartner BL (1996) Between- and within-tree variation in the anatomy and specific gravity of
515 wood in Oregon white oak (*Quercus garryana* Dougl.). *IAWA J* 17:445–461. doi: 10.1163/22941932-90000642

516 Lei Y, Liu Y, Song H, Sun B (2014) A wetness index derived from tree-rings in the Mt. Yishan area of China
517 since 1755 AD and its agricultural implications. *Chin Sci Bull* 59(27):3449–3456. doi: 10.1007/s11434-014-0410-7

518 Li X, Liang E, Gričar J, Prislan P, Rossi S, Čufar K (2013) Age dependence of xylogenesis and its climatic
519 sensitivity in Smith fir on the south-eastern Tibetan Plateau. *Tree Physiol* 33(1)–48–56. doi: 10.1093/treephys/tps113

520 Nicholls JWP, Waring HD (1977) The effect of environmental factors on wood characteristics. IV. Irrigation and
521 partial droughting of *Pinus radiata*. *Silvae Genet* 26:107–111.

522 Olano JM, Eugenio M, García-Cervigón AI, Folch M, Rozas V (2012) Quantitative tracheid anatomy reveals a
523 complex environmental control of wood structure in continental Mediterranean climate. *Int J Plant Sci* 173(2):137–149.
524 doi: 10.1086/663165

525 Overdieck D (2016) *CO₂, temperature, and trees*. Springer, Singapore.

526 Pacheco A, Camarero JJ, Carrer M (2016). Linking wood anatomy and xylogenesis allows pinpointing of climate
527 and drought influences on growth of coexisting conifers in continental Mediterranean climate. *Tree Physiol* 36:502–512.
528 doi: 10.1093/treephys/tpv125

529 Panyushkina IP, Hughes MK, Vaganov EA, Munro MA (2003) Summer temperature in northeastern Siberia since
530 1642 reconstructed from tracheid dimensions and cell numbers of *Larix cajanderi*. *Can J For Res* 33(10):1905–1914. doi:
531 10.1139/x03-109

532 Pérez-de-Lis G, Rossi S, Vázquez-Ruiz RA, Rozas V, García-González I (2016) Do changes in spring phenology
533 affect earlywood vessels? Perspective from the xylogenesis monitoring of two sympatric ring-porous oaks. *New Phytol*
534 209(2):521-530. doi: 10.1111/nph.13610

535 Peters RL, Balanzategui D, Hurley AG, von Arx G, Prendin AL, Cuny HE et al (2018) RAPTOR: Row and
536 position tracheid organizer in R. *Dendrochronologia* 47:10–16. doi: 10.1016/j.dendro.2017.10.003

537 Petterle A, Karlberg A, Bhalerao RP (2013) Daylength mediated control of seasonal growth patterns in perennial
538 trees. *Curr Opin Plant Biol* 16(3):301–306. doi: 10.1016/j.pbi.2013.02.006

539 Popkova MI, Tychkov II, Babushkina EA, Shishov VV (2015) A modified algorithm for estimating the radial cell
540 size in the Vaganov-Shashkin simulation model. *J SibFU Biol* 4(8):495–513. doi: 10.17516/1997-1389-2015-8-4-495-513

541 Popkova MI, Vaganov EA, Shishov VV, Babushkina EA, Rossi S, Bryukhanova MV, Fonti P (2018) Modeled
542 tracheidograms disclose drought influence on *Pinus sylvestris* tree-rings structure from Siberian forest-steppe. *Front Plant*
543 *Sci* 9:1144. doi: 10.3389/fpls.2018.01144

544 Prendin AL, Petit G, Carrer M, Fonti P, Björklund J, von Arx G (2017) New research perspectives from a novel
545 approach to quantify tracheid wall thickness. *Tree Physiol* 37(7):976–983. doi: 10.1093/treephys/tpx037

546 Prislán P, Gričar J, de Luis M, Smith KT, Čufar K (2013) Phenological variation in xylem and phloem formation
547 in *Fagus sylvatica* from two contrasting sites. *Agric For Meteorol* 180:142–151. doi: 10.1016/j.agrformet.2013.06.001

548 Pritzkow C, Heinrich I, Grudh H, Helle G (2014) Relationship between wood anatomy, tree-ring widths and wood
549 density of *Pinus sylvestris* L. and climate at high latitudes in northern Sweden. *Dendrochronologia* 32:295–302. doi:
550 10.1016/j.dendro.2014.07.003 1125-7865

551 Puchałka R, Koprowski M, Przybylak J, Przybylak R, Dąbrowski HP (2016) Did the late spring frost in 2007 and
552 2011 affect tree-ring width and earlywood vessel size in Pedunculate oak (*Quercus robur*) in northern Poland? *Int J*
553 *Biometeorol* 60(8):1143–1150. doi: 10.1007/s00484-015-1107-6

554 Rathgeber CB, Cuny HE, Fonti P (2016) Biological basis of tree-ring formation: a crash course. *Front Plant*
555 *Science* 7:734. doi: 10.3389/fpls.2016.00734

556 Rathgeber CB (2017) Conifer tree-ring density inter-annual variability—anatomical, physiological and
557 environmental determinants. *New Phytol* 216(3):621–625. doi: 10.1111/nph.14763

558 Ren P, Rossi S, Gricar J, Liang E, Cufar K (2015) Is precipitation a trigger for the onset of xylogenesis in
559 *Juniperus przewalskii* on the north-eastern Tibetan Plateau? *Ann Bot* 115(4):629–639. doi: 10.1093/aob/mcu259

560 Ren P, Rossi S, Camarero JJ, Ellison AM, Liang E, Peñuelas J (2018) Critical temperature and precipitation
561 thresholds for the onset of xylogenesis of *Juniperus przewalskii* in a semi-arid area of the north-eastern Tibetan Plateau.
562 *Ann Bot* 121(4):617–624. doi: 10.1093/aob/mcx188

563 Rossi S, Deslauriers A, Anfodillo T (2006) Assessment of cambial activity and xylogenesis by microsampling tree
564 species: an example at the Alpine timberline. *IAWA J* 27(4):383–394. doi: 10.1163/22941932-90000161

565 Rossi S, Deslauriers A, Anfodillo T, Carrer M (2008). Age-dependent xylogenesis in timberline conifers. *New*
566 *Phytol* 177:199–208. doi: 10.1111/j.1469-8137.2007.02235.x

567 Rossi S, Morin H, Deslauriers A (2012) Causes and correlations in cambium phenology: towards an integrated
568 framework of xylogenesis. *J Exp Bot* 63(5): 2117–2126. doi: 10.1093/jxb/err423

569 Rossi S, Girard M-J, Morin H (2014) Lengthening of the duration of xylogenesis engenders disproportionate
570 increases in xylem production. *Glob Chang Biol* 20:2261–2271. doi: 10.1111/gcb.12470

571 Selyaninov GT (1937) Methods of climate description to agricultural purposes. In: Selyaninov GT (ed.) *World*
572 *climate and agriculture handbook*. pp. 5–27. Gidrometeoizdat, Leningrad (**In Russian**)

573 Seo JW, Eckstein D, Jalkanen R, Rickebusch S, Schmitt U (2008) Estimating the onset of cambial activity in Scots
574 pine in northern Finland by means of the heat-sum approach. *Tree Physiol* 28(1):105–112. doi: 10.1093/treephys/28.1.105

575 Seo JW, Smiljanić M, Wilmking M (2014) Optimizing cell-anatomical chronologies of Scots pine by stepwise
576 increasing the number of radial tracheid rows included – Case study based on three Scandinavian sites. *Dendrochronologia*
577 32(3):205–209. doi: 10.1016/j.dendro.2014.02.002

578 Silkin PP (2010) *Methods of multiparameter analysis of conifers tree-rings structure*. Siberian Federal University,
579 Krasnoyarsk (**In Russian**)

580 Singh SR, Dalal S, Singh R, Dhawan AK., Kalia RK (2012) Seasonal influences on in vitro bud break in
581 *Dendrocalamus hamiltonii* Arn. ex Munro nodal explants and effect of culture microenvironment on large scale shoot
582 multiplication and plantlet regeneration. *Ind J Plant Physiol* 17:9–21.

583 Singh ND, Yadav RR, Venugopal N, Singh V, Yadava AK, Misra KG et al (2016) Climate control on ring width
584 and intra-annual density fluctuations in *Pinus kesiya* growing in a sub-tropical forest of Manipur, Northeast India. *Trees*
585 30(5):1711–1721. doi: 10.1007/s00468-016-1402-9

586 Sterck FJ, Zweifel R, Sass-Klaassen U, Chowdhury Q (2008) Persisting soil drought reduces leaf specific
587 conductivity in Scots pines (*Pinus sylvestris*) and pubescent oak (*Quercus pubescens*). *Tree Physiol* 28(4):528–536. doi:
588 10.1093/treephys/28.4.529

589 Stine AR, Huybers P (2017) Implications of Liebig’s law of the minimum for tree-ring reconstructions of climate.
590 *Environ Res Lett* 12(11):114018. doi: 10.1088/1748-9326/aa8cd6

591 Stokes MA and Smiley TL (1968) An introduction to tree-ring dating. University of Chicago Press, Chicago.

592 Sun Y, Wang L, Yin H (2016) Influence of climatic factors on tree-ring maximum latewood density of *Picea*
593 *schrenkiana* in Xinjiang, China. *Front Earth Sci* 10(1):126–134. doi: 10.1007/s11707-015-0507-6

594 Swidrak I, Gruber A, Oberhuber W (2014) Xylem and phloem phenology in co-occurring conifers exposed to
595 drought. *Trees* 28(4):1161–1171. doi: 10.1007/s00468-014-1026-x

596 Vaganov EA, Shashkin AV, Sviderskaya IV, Vysotskaya LG (1985) Histometric analysis of the woody plants
597 growth. Nauka, Novosibirsk. **(In Russian)**

598 Vaganov EA, Hughes MK, Shashkin AV (2006) Growth dynamics of conifer tree rings: images of past and future
599 environments. Springer, Dordrecht. doi: 10.1007/3-540-31298-6

600 Vaganov EA, Anchukaitis KJ, Evans M (2011) How well understood are the processes that create dendroclimatic
601 records? A mechanistic model of the climatic control on conifer tree-ring growth dynamics. In: Hughes MK, Swetnam TW,
602 Diaz HF (eds) *Dendroclimatology: progress and prospects*. pp 37–75. Springer, Dordrecht. doi: 10.1007/978-1-4020-5725-
603 0_3

604 Venegas-González A, von Arx G, Chagas MP, Filho MT (2015) Plasticity in xylem anatomical traits of two
605 tropical species in response to intra-seasonal climate variability. *Trees* 29(2):423–435. doi: 10.1007/s00468-014-1121-z

606 Vysotskaya LG, Vaganov EA (1989) Components of the variability of radial cell-size in tree rings of conifers.
607 *IAWA Bull* 10:417–428.

608 Wang H, Shao X, Fang X, Jiang Y, Liu C, Qiao Q (2017) Relationships between tree-ring cell features of *Pinus*
609 *koraiensis* and climate factors in the Changbai Mountains, Northeastern China. *J For Res* 28(1): 105–114. doi:
610 10.1007/s11676-016-0292-4

611 Wheeler EA, Baas P (1993) The potentials and limitations of dicotyledonous wood anatomy for climatic
612 reconstructions. *Paleobiol* 19(4):487–498. doi: 10.1017/S009483730001410X

613 Wigley TML, Briffa KR, Jones PD (1984) On the average value of correlated time series, with application in
614 dendrochronology and hydrometeorology. *J Clim Appl Meteorol* 23:201–213. doi: 10.1175/1520-
615 0450(1984)023<0201:OTAVOC>2.0.CO;2

616 Wilkinson S, Ogée J, Domec JC, Rayment M, Wingate L (2015) Biophysical modelling of intra-ring variations in
617 tracheid features and wood density of *Pinus pinaster* trees exposed to seasonal droughts. *Tree Phys* 35(3): 305–318. doi:
618 10.1093/treephys/tpv010

619 Wimmer R, Strumia G, Holawe F (2000) Use of false rings in Austrian pine to reconstruct early growing season
620 precipitation. *Can J For Res* 30(11):1691–1697. doi: 10.1139/x00-095

621 Wimmer R (2002) Wood anatomical features in tree-rings as indicators of environmental change.
622 *Dendrochronologia* 20(1-2):21–36. doi: 10.1078/1125-7865-00005

623 Yang B, He M, Shishov V, Tychkov I, Vaganov E, Rossi S et al (2017) New perspective on spring vegetation
624 phenology and global climate change based on Tibetan Plateau tree-ring data. *PNAS* 114(27):6966–6971. doi:
625 10.1073/pnas.1616608114

626 Yasue K, Funada R, Kobayashi O, Ohtani J (2000) The effects of tracheid dimensions on variations in maximum
627 density of *Picea glehnii* and relationships to climatic factors. *Trees* 14(4):223–229. doi: 10.1007/PL00009766

628 Zalloni E, de Luis M, Campelo F, Novak K, De Micco V, Di Filippo A et al (2016) Climatic signals from intra-
629 annual density fluctuation frequency in Mediterranean pines at a regional scale. *Front Plant Sci*, 7:579. doi:
630 10.3389/fpls.2016.00579

631 Ziaco E, Biondi F (2016) Tree growth, cambial phenology, and wood anatomy of limber pine at a Great Basin
632 (USA) mountain observatory. *Trees* 30(5):1507–1521. doi: 10.1007/s00468-016-1384-7

633 Ziaco E, Biondi F, Heinrich I (2016) Wood cellular dendroclimatology: testing new proxies in Great Basin
634 bristlecone pine. *Front Plant Sci* 7:1602. doi: 10.3389/fpls.2016.01602

635 Ziaco E, Truettner C, Biondi F, Bullock S (2018) Moisture-driven xylogenesis in *Pinus ponderosa* from a Mojave
636 Desert mountain reveals high phenological plasticity. *Plant Cell Environ* 41(4):823–836. doi: 10.1111/pce.13152

637

638 **Table 1** Comparison of individual tree xylem anatomical parameters between pine and larch species. CD_{mean1} , mean cell
639 radial diameter, calculated as slope of linear regression TRW(N); R^2 , determination coefficient of linear regression
640 TRW(N); CD_{mean2} , arithmetic mean for individual tree series of mean cell radial diameter; N_{mean} , arithmetic mean for
641 individual tree series of cell number per ring

Individual tree characteristics	Pine trees					Larch trees				
	PS01	PS08	PS05	PS02	PS07	LS11	LS15	LS16	LS13	LS12
CD_{mean1} (μm)	42.11	41.33	39.11	35.66	33.97	43.65	42.61	40.58	32.98	31.69
R^2	0.94	0.92	0.99	0.96	0.97	0.91	0.94	0.99	0.94	0.90
CD_{mean2} (μm)	40.05	38.50	33.42	33.72	28.94	41.71	35.94	32.34	32.36	31.59
N_{mean}	44.0	31.5	20.8	50.0	43.4	17.6	16.5	11.8	13.7	22.3

642

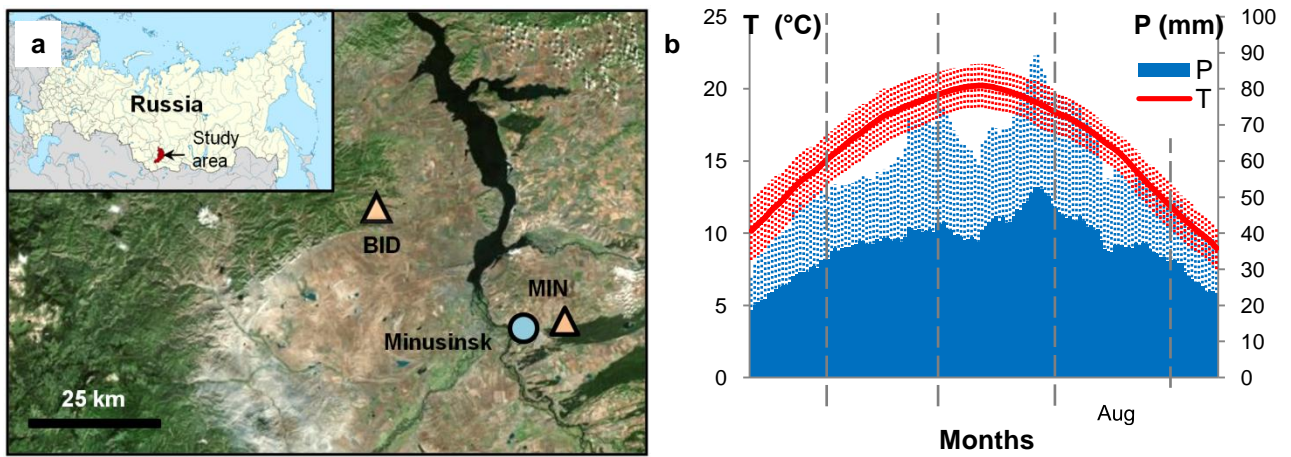


Fig. 1 Location and climate of study area: (a) Map of the central part of Minusinsk depression and position of the study area in Russia (upper-left corner insert). Triangles indicate location of tree-ring sampling sites. Circle is Minusinsk weather station. (b) Climograph of growing season May-September on the Minusinsk weather station for 1964–2011. Red is mean temperature (T) and blue is sum of precipitation (P) calculated from daily data with a 20-day moving window and 1-day step. Vertical red and blue lines are standard deviations of the inter-annual climatic series

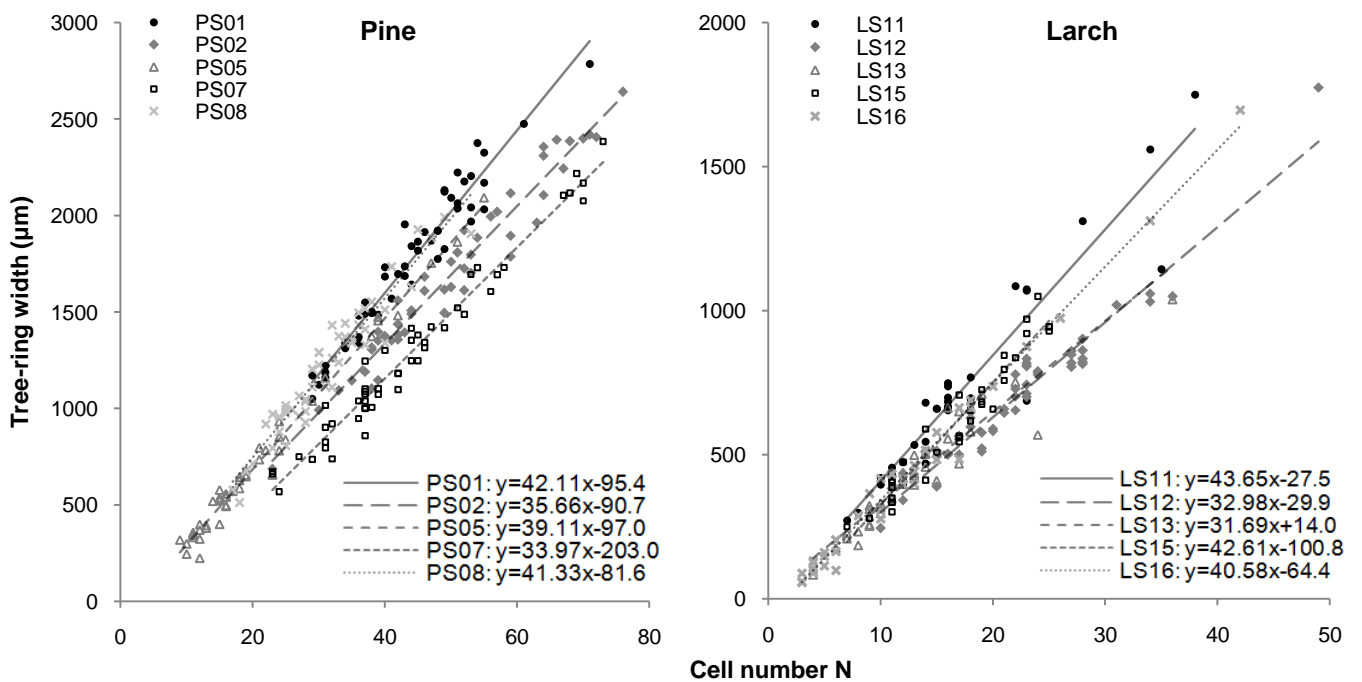
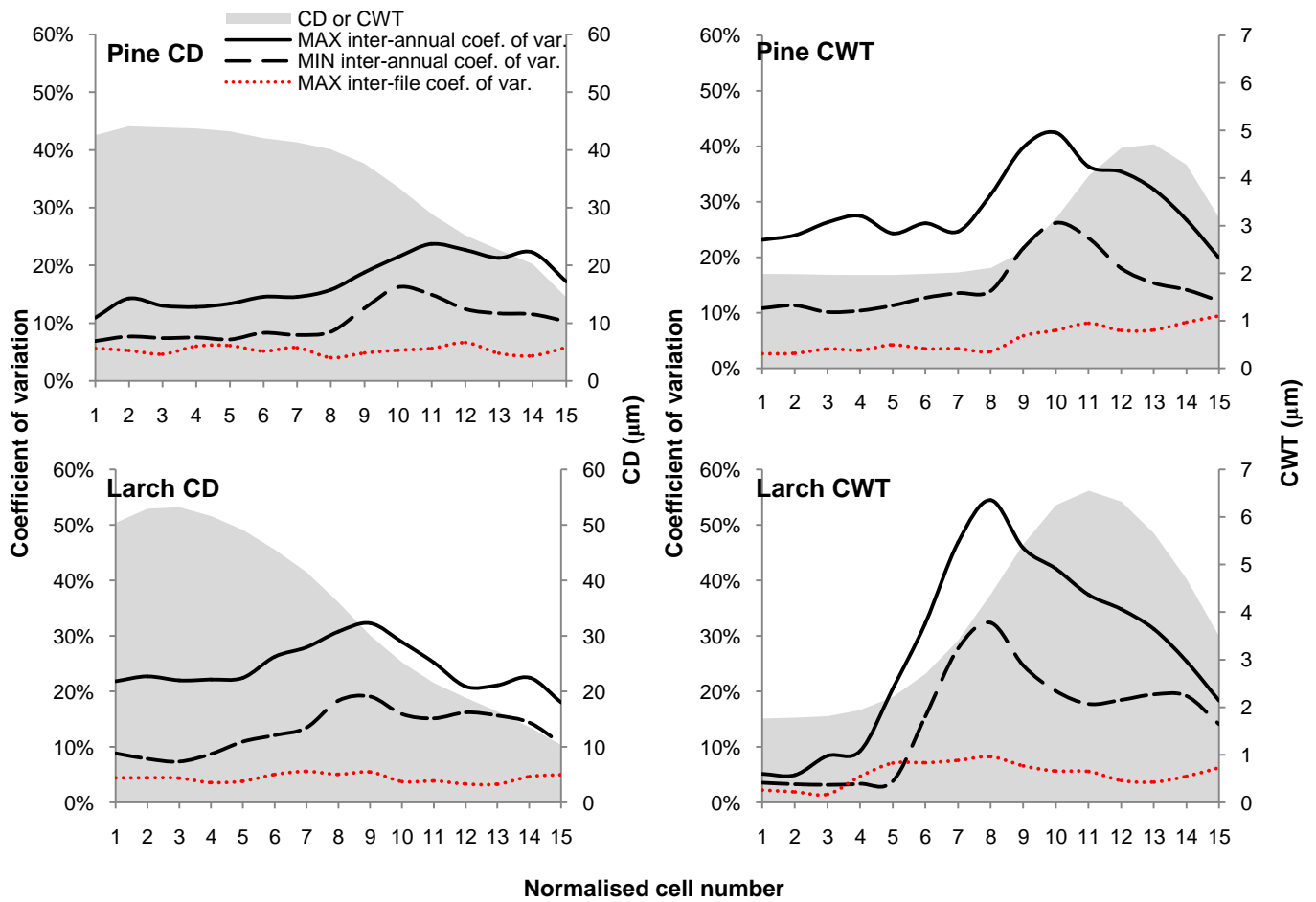


Fig. 2 Scatterplots of tree-ring width and cell number in the raw measurements of individual tree series. Lines show linear regression functions calculated for each tree



Normalised cell number

Fig. 3 Tracheidograms of pine and larch cell parameters normalised to 15 cells per ring and their variation. The pattern of inter-annual variation of cell parameters' series was calculated for each individual tree separately; its ranges (maximal and minimal values of the coefficient of variation among individual tree series for each normalised cell number) are delineated with solid and dashed lines (see legend on the top). Dotted red line is the maximum value of inter-file coefficient of variation calculated during diagnostic test for the number of replications (ESM). Left Y-axis is coefficient of variation (lines) and right Y-axis is value of the studied cell parameter (grey shade): CD, cell radial diameter; CWT, cell wall thickness

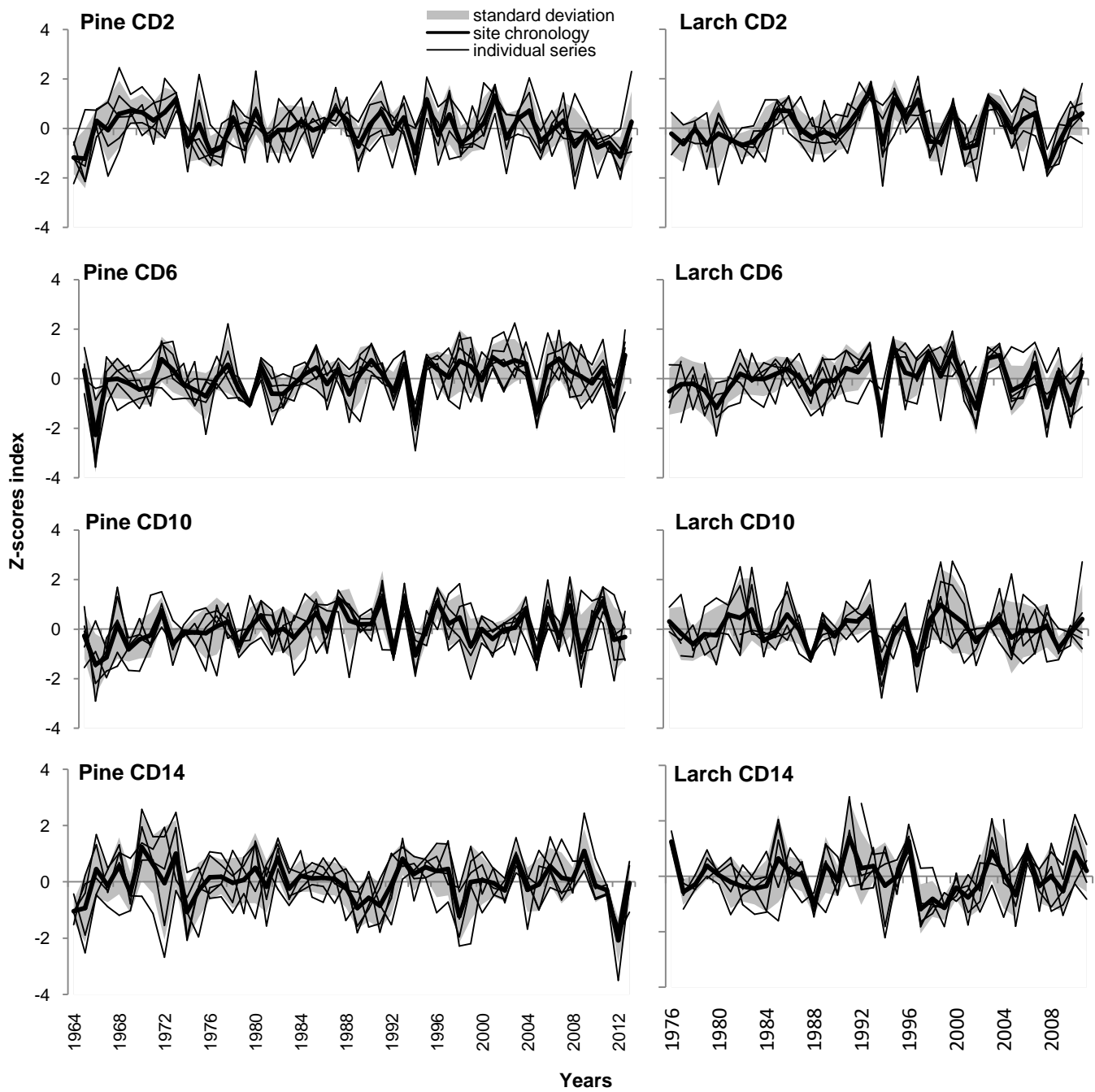


Fig. 4 Z-scores of individual series (thin lines) and site chronologies (thick line) of cell radial diameters (CD) for some of normalised cells: 2nd, 6th, 10th and 14th. Standard deviation (grey shade) was calculated for CD of five individual trees for each year separately

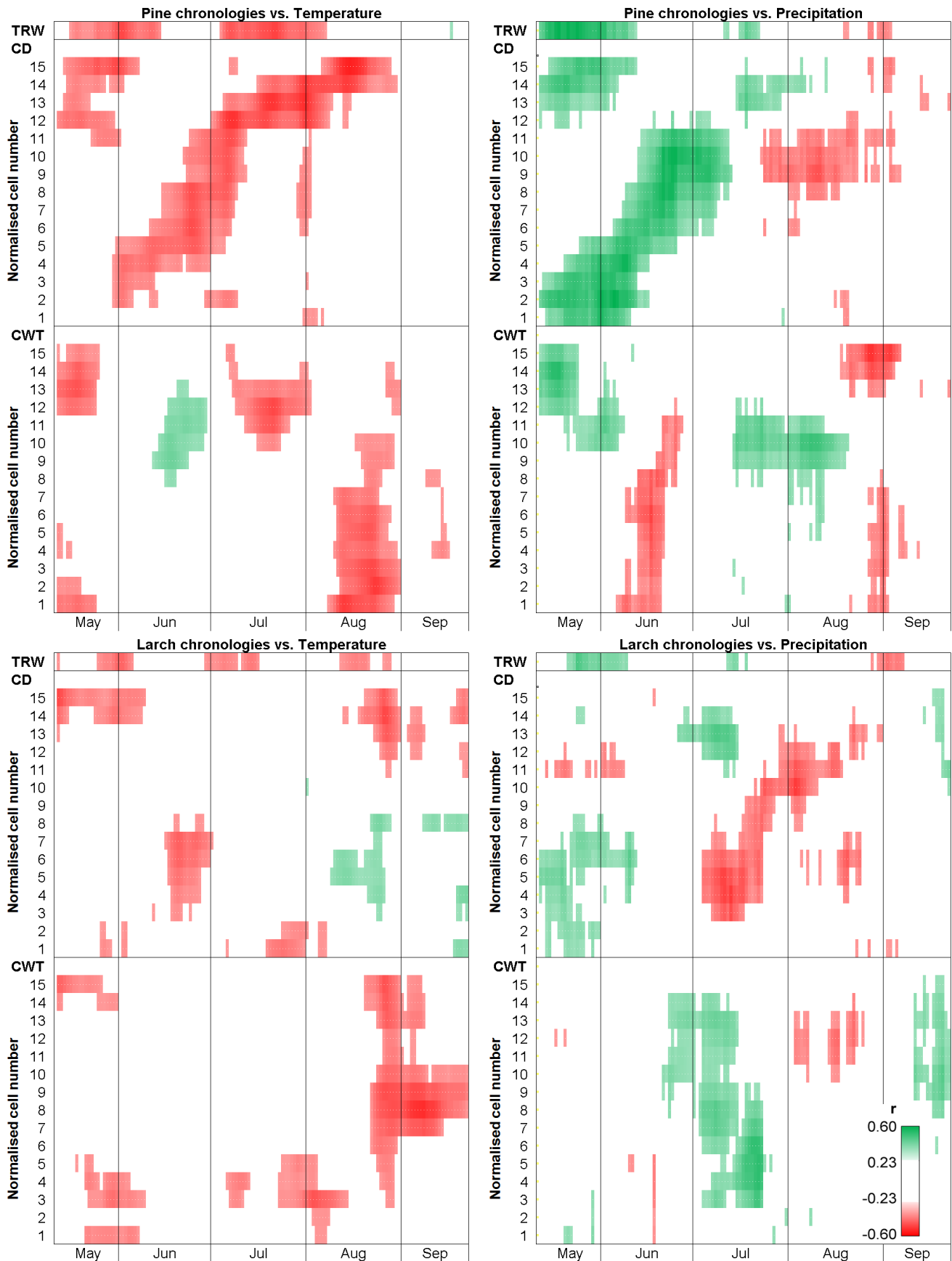


Fig. 5 Correlation coefficients between the site chronologies of tree-ring parameters and 20-day moving series of temperature and precipitation. TRW, ring width indexed chronology; CD, cell radial diameter; CWT, cell wall thickness. Correlation bar is shown at the low right corner of the last plot. Green is positive and red is negative correlation. Only significant correlations at $P \leq 0.05$ are shown

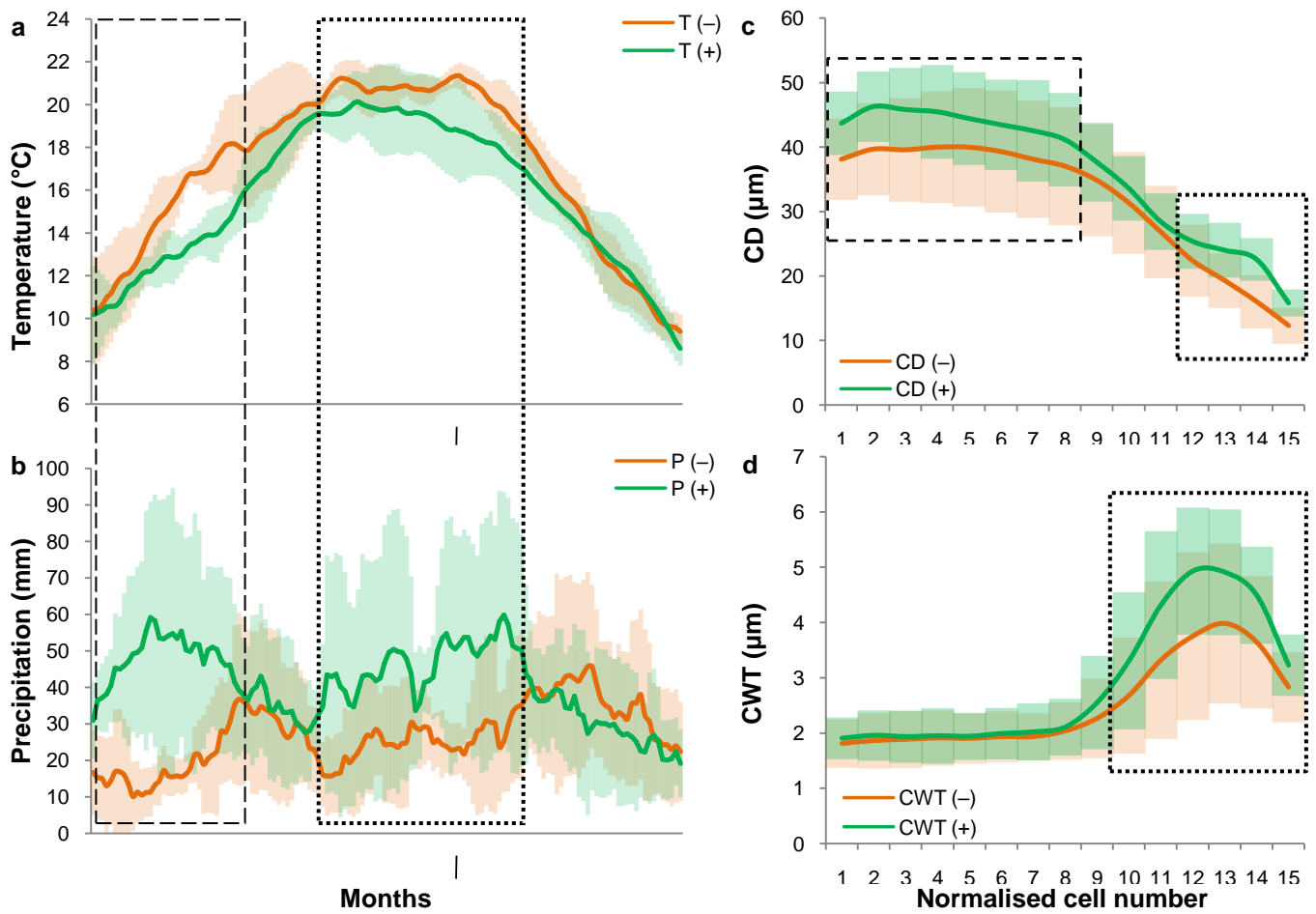


Fig. 6 Variations of (a) temperature and (b) precipitation, and (c) radial cell diameters (CD) and (d) cell-wall thickness (CWT) of pine during negative (orange) and positive (green) pointer years. May to September climographs (a and b) are calculated from the Minusinsk daily data with a 20-day moving window. Tracheidograms (c and d) show fluctuations of cell parameters within 15-cell normalised ring. Lines mark the mean values and shades are $\pm 1 \sigma$ range of studied parameters. Rectangles indicate the intervals with the significant at $P < 0.05$ differences between positive and negative pointer years

ELECTRONIC SUPPLEMENTARY MATERIALS

The materials include the details for selection of a constant cell number (also called normalised cell number) applied to the cell measurements, normalisation procedure, and testing of replication number of file measurements. Additionally, there are four tables and three figures to support the narrative and arguments of this paper.

Selecting the constant cell number for normalisation of cell measurements

The cell number varies both between rings and within a ring. For comparison of the anatomical parameters between rings and samples, the measured cell series need to be converted to a constant number of cells. There is no standard methodological approach for the cell measurement normalisation in the quantitative wood anatomy research. The procedure of normalisation of the cell dimensions within the tree ring and tracheidogram calculation are described by Terskov et al. (1981) and Vaganov (1990). Some wood anatomical studies used the average number of cells per ring in the investigated sample to normalise the cell data (Panyushkina et al. 2003; Deslauriers and Morin 2005; Ziaco and Biondi 2016). Other researchers received reliable results by dividing a ring into the fixed number of 10 zones disregarding the actual cell number (Carrer et al. 2017; Castagneri et al. 2017).

All these approaches to cell normalisation are challenged by the possible distortion of climatic signals imprinted into various parts (zones) of a ring. In case when a normalising procedure stretches a tracheidogram too much, measurement of one actual tracheid is being put into several adjacent normalised cell positions. This may cause a distortion in the temporal window of climatic signal of normalised cell chronologies. Additionally, a large number of normalised cells results in a dramatic increase in the size of cell data set to be analysed. In contrast, tracheidogram compression aggregates the climatic signal of consecutive cells prompting higher correlations with climatic factors, and strengthening and isolating the temporal window of signal. Because the goal of this study is to investigate the intra-ring variation of climatic signals, we avoid stretching tracheidograms and use the lesser of two site average cell numbers for normalising. The average cell number is about 15 cells for the larch samples and 40 cells for pine samples. We normalise the cell measurements to the constant number of $c = 15$ cells. The normalised tracheidograms will be mostly compressed, and the percent of rings stretched more than twice is only ca. 10% for larch samples and zero for pine.

Normalisation of cell measurements

We applied normalisation technique described by Vaganov (1990). This procedure operates on raw tracheidogram. A raw tracheidogram is a sequence of measured values for each cell in the ring radial file $\{X_i\}$, $i = 1, \dots, N$, where X is cell parameter (CD or CWT in this study); N is number of cells in measured radial file. The normalising procedure consists of two steps. Firstly, raw tracheidogram is stretched c times in the intermediate sequence:

$$\{X_i^*\} = \underbrace{X_1, \dots, X_1}_c, \underbrace{X_2, \dots, X_2}_c, \dots, \underbrace{X_N, \dots, X_N}_c, \quad i = 1, \dots, N \cdot c$$

Secondly, intermediate sequence is compressed in the final normalised tracheidogram $\{\hat{X}_i\}$, $i = 1, \dots, c$, where

$$\hat{X}_i = \frac{1}{N} \sum_{j=N \cdot (i-1)+1}^{N \cdot i} X_i^*.$$

After this transformation, tracheidograms of different radial files are averaged, so different rings can be easily compared. This also provides opportunity for developing individual tree series and site chronologies for each normalised cell number and each cell parameter.

Diagnostic test on the number of replicated measurements per a ring

The cell measurements and data normalisation is one of the most time consuming steps of wood anatomy research. Therefore, to select an optimum number of replication for the cell measurements we applied procedure based on Seo et al. (2014) study of Scots pine in quite different environment. We tested the replication of measurements more vigorously. Three rings with cell numbers about 20, 40, and 60 cells were tested at each site, We developed a set of anatomical parameters with 10 files of the replicated measurements (radial files) per a ring and normalised them to the average cell number calculated for each ring separately. Figure S1 demonstrates the results of correlation analyses between the tracheidograms averaged from various number of radial files from 1 to 9 with each other and with the master tracheidogram of all 10 radial files. The comparison indicates that the optimum number of file measurements is five, because the tracheidograms maintain a common pattern in the range of CD and CWT parameters after the five-replication threshold with the mean correlations above 0.9 and 90% confidence level in all tested rings.

We notice that averaging over five files sufficiently reduces inter-files component, but not excludes it completely. An estimate of the maximum residual inter-files variation was carried out for tested three rings used for determination of measured files number. For each ring, inter-files variation was calculated for full set of tracheidograms averaged over random five files out of ten measured files in total.

Table S1 Climate of the study area for the common period of observation 1927-2016

Climatic parameter	Month												Year
	Jan	Feb	Mar	Apr	May	Jun	Jul	Aug	Sep	Oct	Nov	Dec	
Temperature													
average (°C) for MIN	-19.5	-17.5	-7.6	3.6	11.1	17.6	19.9	16.9	9.9	2.1	-8.1	-16.3	1.0
average (°C) for BID	-19.7	-17.7	-8.7	2.5	10.0	16.5	18.7	16.1	10.7	1.7	-9.0	-17.2	0.3
MIN and BID correlation	0.96	0.94	0.97	0.97	0.97	0.96	0.94	0.96	0.96	0.91	0.94	0.96	0.96
Precipitation													
average (mm) for MIN	8.1	7.1	7.1	15.8	33.4	56.1	65.9	58.4	42.1	22.1	14.5	11.1	342
average (mm) for BID	15.6	12.8	16.6	31.0	47.0	64.6	79.2	71.6	53.1	36.0	32.8	25.3	486
MIN and BID correlation	0.84	0.72	0.80	0.89	0.88	0.86	0.89	0.88	0.89	0.82	0.80	0.87	0.80

Minusinsk station (53°41'N 91°40'E) is 15 km from MIN site; gridded observations from CRU TS 4.01 (Harris et al. 2014) are averaged for 53.5°-54.5°N 90.5°-91.5°E grid, in the middle of which BID site is placed, and Minusinsk station and MIN site are located outside of it.

All correlations are significant at $P \leq 0.01$

Table S2 Correlations coefficients of cell parameter inter-annual variation with the mean cell diameter and the mean cell number, calculated for each individual tree. CD, cell radial diameter; CWT, cell wall thickness; CD_{mean1} , mean cell radial diameter for individual tree estimated with TRW(N) linear regression; CD_{mean2} , mean cell radial diameter for individual tree estimated as average of mean cell radial diameters for all measured rings; N_{mean} , mean cell number per ring for individual tree (see Table 1)

Correlated parameters of individual trees		Normalised cell number														
		1	2	3	4	5	6	7	8	9	10	11	12	13	14	15
Pine																
Inter-annual variation of CD series	CD_{mean1}	-0.08	-0.39	-0.47	-0.41	-0.63	-0.75	-0.69	-0.52	-0.18	0.27	0.53	0.01	-0.34	-0.12	-0.18
	CD_{mean2}	-0.39	-0.70	-0.76	-0.72	-0.87	-0.94	-0.88	-0.78	-0.51	-0.02	0.22	-0.35	-0.66	-0.45	-0.46
	N_{mean}	-0.75	-0.62	-0.53	-0.59	-0.39	-0.23	-0.37	-0.55	-0.80	-0.81	-0.98	-0.90	-0.65	-0.80	-0.63
Inter-annual variation of CWT series	CD_{mean1}	-0.31	-0.37	-0.56	-0.49	-0.52	-0.59	-0.47	-0.26	-0.22	-0.76	-0.66	-0.25	-0.12	-0.02	-0.18
	CD_{mean2}	-0.48	-0.54	-0.72	-0.62	-0.63	-0.74	-0.62	-0.34	-0.11	-0.60	-0.87	-0.58	-0.47	-0.38	-0.44
	N_{mean}	-0.29	-0.28	-0.14	-0.12	-0.05	-0.08	-0.03	0.21	0.66	0.77	-0.43	-0.76	-0.80	-0.83	-0.50
Larch																
Inter-annual variation of CD series	CD_{mean1}	0.15	0.11	0.13	-0.04	-0.38	-0.41	-0.34	-0.08	-0.02	0.08	0.32	-0.09	-0.30	-0.40	-0.63
	CD_{mean2}	-0.32	-0.38	-0.38	-0.60	-0.85	-0.81	-0.83	-0.68	-0.37	-0.18	-0.24	-0.51	-0.59	-0.31	-0.40
	N_{mean}	-0.93	-0.91	-0.88	-0.74	-0.28	-0.15	-0.13	-0.63	-0.96	-0.98	-0.85	-0.38	0.34	0.83	0.74
Inter-annual variation of CWT series	CD_{mean1}	-0.76	-0.87	-0.79	-0.14	0.07	-0.16	0.25	0.62	0.60	0.34	0.28	0.14	0.11	-0.03	-0.72
	CD_{mean2}	-0.68	-0.74	-0.64	-0.60	-0.55	-0.53	-0.26	0.12	0.18	-0.09	-0.21	-0.36	-0.52	-0.65	-0.70
	N_{mean}	0.62	0.47	0.66	0.59	0.43	0.33	0.31	-0.45	-0.82	-0.97	-0.95	-0.93	-0.73	-0.28	0.63

Bold correlation coefficients are significant at $P \leq 0.05$

Table S3 Coefficient of inter-annual variation (%) for the site chronologies of cell parameters of pine and larch. CD, cell radial diameter, CWT, cell wall thickness

Cell parameter	Normalised cell number														
	1	2	3	4	5	6	7	8	9	10	11	12	13	14	15
Pine															
CD	6.1	6.6	6.2	5.7	6.7	7.6	8.5	8.9	9.8	11.7	10.4	8.6	9.6	10.6	8.5
CWT	10.7	11.1	10.5	13.0	16.6	17.7	20.0	19.9	17.1	12.8	13.4	17.4	18.3	19.5	13.4
Larch															
CD	8.1	8.2	7.1	7.4	7.2	7.5	7.4	9.6	16.8	21.1	17.8	14.1	12.6	11.1	8.2
CWT	2.0	2.0	2.5	4.9	9.6	12.2	24.2	25.2	25.3	22.1	20.0	18.2	17.0	15.0	9.5

Table S4 Mean correlation coefficients between individual series of cell parameters and respective site chronologies. CD, cell radial diameter, CWT, cell wall thickness

Cell parameter	Normalised cell number														
	1	2	3	4	5	6	7	8	9	10	11	12	13	14	15
Pine															
CD	0.65	0.64	0.62	0.58	0.66	0.69	0.73	0.71	0.66	0.66	0.58	0.55	0.61	0.63	0.59
CWT	0.44	0.45	0.39	0.39	0.42	0.39	0.39	0.40	0.51	0.58	0.58	0.58	0.59	0.55	0.50
Larch															
CD	0.70	0.74	0.73	0.75	0.76	0.71	0.70	0.67	0.64	0.59	0.65	0.72	0.67	0.63	0.53
CWT	0.46	0.53	0.46	0.35	0.31	0.33	0.48	0.60	0.66	0.67	0.70	0.70	0.69	0.67	0.62

All correlations are significant at $P \leq 0.05$

Table S5 Correlation coefficients between cell diameter site chronologies of different normalised cell numbers

		Normalised cell number														
		1	2	3	4	5	6	7	8	9	10	11	12	13	14	15
Pine	1															
	2	0.81														
	3	0.68	0.83													
	4	0.63	0.73	0.88												
	5	0.47	0.52	0.64	0.80											
	6	0.27	0.42	0.53	0.65	0.84										
	7	0.22	0.38	0.41	0.54	0.72	0.92									
	8	0.20	0.37	0.35	0.47	0.65	0.86	0.94								
	9	0.13	0.27	0.28	0.40	0.58	0.72	0.80	0.90							
	10	0.08	0.15	0.22	0.30	0.48	0.56	0.64	0.75	0.90						
	11	0.05	0.14	0.20	0.20	0.38	0.41	0.50	0.58	0.73	0.89					
	12	0.23	0.37	0.32	0.23	0.36	0.37	0.42	0.49	0.52	0.53	0.71				
	13	0.38	0.51	0.37	0.26	0.24	0.23	0.27	0.30	0.24	0.14	0.27	0.81			
	14	0.40	0.51	0.44	0.37	0.27	0.22	0.24	0.27	0.19	0.09	0.18	0.61	0.88		
	15	0.27	0.43	0.38	0.43	0.35	0.28	0.28	0.33	0.29	0.18	0.27	0.49	0.64	0.84	
Larch	1															
	2	0.93														
	3	0.78	0.89													
	4	0.58	0.68	0.89												
	5	0.32	0.44	0.69	0.89											
	6	0.27	0.37	0.58	0.79	0.94										
	7	0.41	0.48	0.57	0.68	0.76	0.89									
	8	0.33	0.39	0.42	0.50	0.53	0.66	0.87								
	9	0.15	0.20	0.19	0.24	0.31	0.41	0.62	0.88							
	10	0.07	0.10	0.11	0.11	0.15	0.21	0.42	0.69	0.88						
	11	0.02	0.03	0.02	-0.05	-0.05	-0.02	0.09	0.26	0.47	0.70					
	12	0.08	0.04	-0.02	-0.17	-0.15	-0.12	-0.05	0.06	0.24	0.48	0.88				
	13	0.11	0.07	0.02	-0.18	-0.19	-0.16	-0.10	-0.02	0.12	0.35	0.73	0.91			
	14	0.10	0.11	0.06	-0.21	-0.19	-0.19	-0.13	-0.08	0.08	0.22	0.46	0.66	0.86		
	15	-0.05	-0.03	-0.08	-0.33	-0.28	-0.28	-0.22	-0.12	0.09	0.21	0.38	0.51	0.67	0.88	

Shade indicates correlations for which $R^2 > 0.5$ (more than half of common variance). Bold correlation coefficients are significant at $P \leq 0.05$

Table S6 Correlation coefficients between cell wall thickness site chronologies of different normalised cell numbers

		Normalised cell number														
		1	2	3	4	5	6	7	8	9	10	11	12	13	14	15
Pine	1															
	2	0.90														
	3	0.81	0.94													
	4	0.74	0.85	0.93												
	5	0.75	0.83	0.91	0.94											
	6	0.70	0.79	0.85	0.86	0.92										
	7	0.70	0.75	0.77	0.81	0.85	0.92									
	8	0.48	0.59	0.67	0.72	0.73	0.77	0.87								
	9	0.27	0.40	0.49	0.53	0.50	0.51	0.62	0.86							
	10	0.22	0.33	0.40	0.43	0.42	0.40	0.52	0.75	0.93						
	11	0.29	0.39	0.41	0.42	0.43	0.40	0.50	0.63	0.76	0.90					
	12	0.32	0.37	0.36	0.37	0.38	0.39	0.48	0.51	0.59	0.71	0.90				
	13	0.41	0.45	0.42	0.42	0.40	0.43	0.48	0.42	0.44	0.51	0.71	0.91			
	14	0.42	0.41	0.35	0.33	0.34	0.36	0.38	0.26	0.27	0.30	0.51	0.76	0.91		
	15	0.31	0.28	0.21	0.18	0.21	0.23	0.22	0.09	0.08	0.09	0.27	0.53	0.71	0.89	
Larch	1															
	2	0.90														
	3	0.61	0.56													
	4	0.26	0.11	0.81												
	5	0.27	0.11	0.76	0.94											
	6	0.24	0.10	0.63	0.79	0.92										
	7	0.17	0.12	0.47	0.56	0.67	0.86									
	8	0.08	0.08	0.35	0.37	0.43	0.61	0.88								
	9	-0.03	-0.01	0.23	0.25	0.29	0.41	0.64	0.91							
	10	-0.05	0.00	0.15	0.19	0.21	0.29	0.47	0.74	0.92						
	11	-0.04	0.01	0.12	0.16	0.16	0.21	0.35	0.57	0.76	0.94					
	12	-0.07	-0.03	0.13	0.21	0.22	0.23	0.33	0.50	0.67	0.86	0.97				
	13	-0.04	-0.01	0.19	0.28	0.30	0.31	0.39	0.55	0.69	0.84	0.89	0.95			
	14	-0.04	-0.04	0.22	0.28	0.31	0.31	0.35	0.51	0.64	0.76	0.78	0.84	0.95		
	15	-0.01	-0.01	0.27	0.28	0.30	0.29	0.30	0.41	0.52	0.58	0.58	0.64	0.76	0.89	

Shade indicates correlations for which $R^2 > 0.5$ (more than half of common variance). Bold correlation coefficients are significant at $P \leq 0.05$

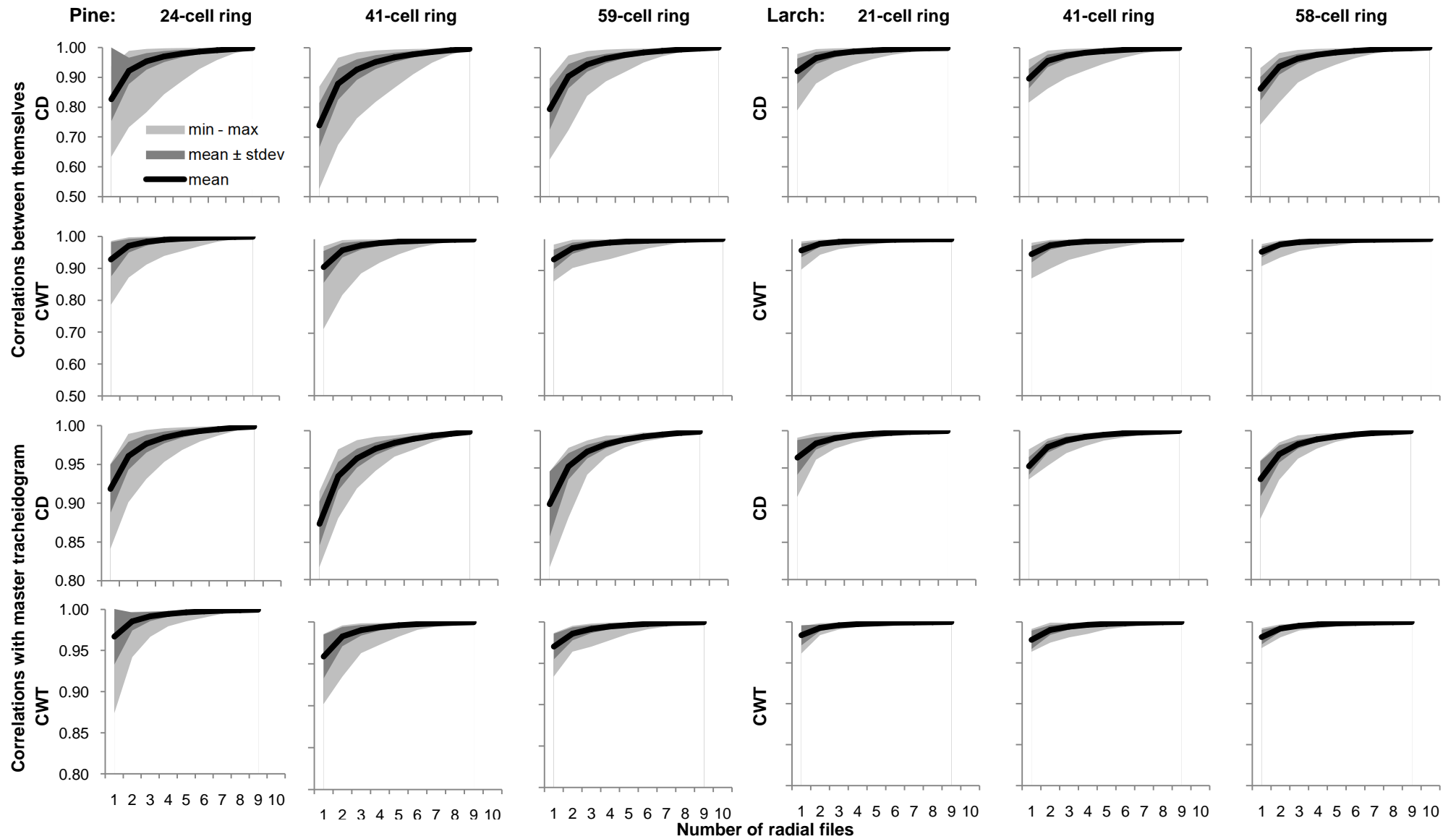


Figure S1 Results of diagnostic test for the range of correlations of the cell parameters' tracheidograms averaged from different number of randomly selected radial files of cells (from 1 to 9) between themselves (top two rows of panels), and their correlations with master tracheidogram averaged by all ten measured radial files (bottom two rows of panels). Cell number of tested rings is shown above top panels. CD, cell radial diameter, CWT, cell wall thickness

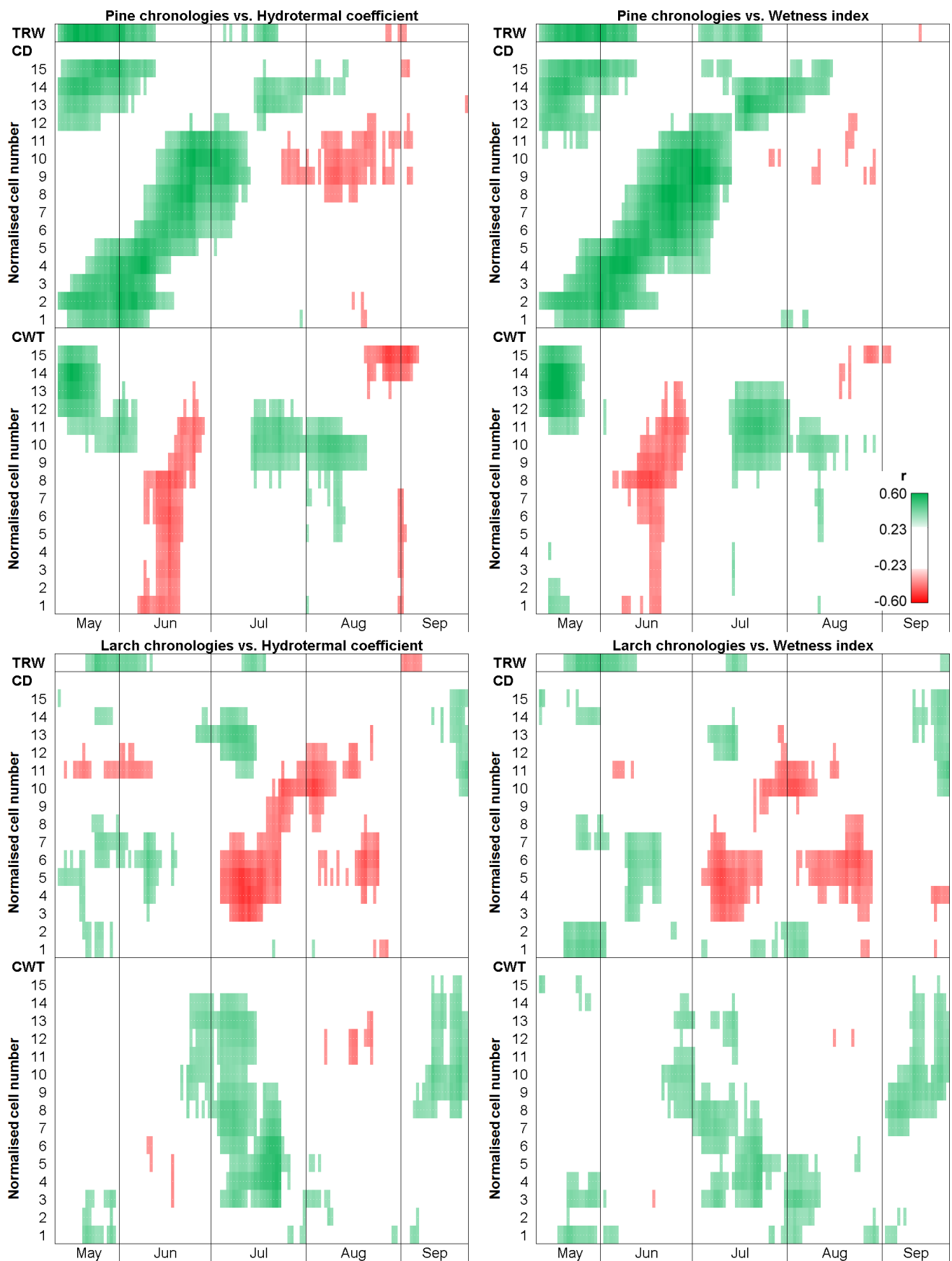


Figure S2. Correlation coefficients between the site chronologies of tree-ring parameters and 20-day moving series of moisture regime indices. TRW, ring width indexed chronology; CD, cell radial diameter; CWT, cell wall thickness. Correlation bar is shown at the low right corner of the last plot. Green is positive and red is negative correlation. Only significant correlations at $P \leq 0.05$ are shown

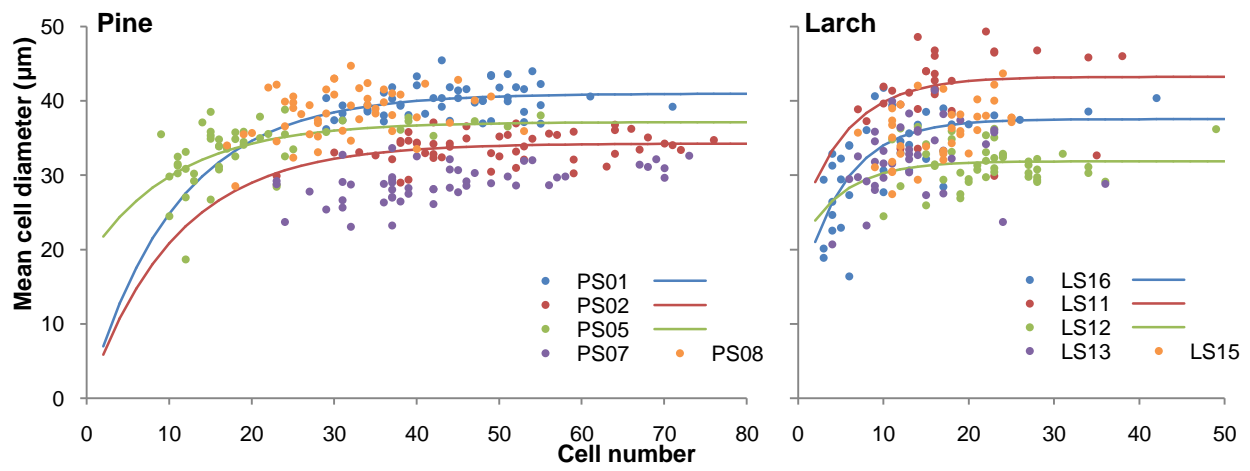


Figure S3. Relationship between the mean cell diameter and the cell number per ring. Scatterplots represent non-normalized (raw) measurements for pine and larch. Lines show approximation exponential functions calculated for some individual trees as described in Babushkina (2011). Colours represent individual trees (see the legend)

References

- Harris I, Jones PD, Osborn TJ, Lister DH (2014) Updated high-resolution grids of monthly climatic observations – the CRU TS3.10 Dataset. *Int J Climatol* 34:623–642. doi: 10.1002/joc.3711
- Terskov IA, Vaganov EA, Sviderskaya IV (1981) Tracheidograms of tree rings as characteristics of seasonal growth rate. *Izv SO RAN Ser Biol* 2:22–30. (in Russian)
- Vaganov EA (1990) The tracheidogram method in tree-ring analysis and its application. In: Cook ER, Kairiukstis LA (eds) *Methods of Dendrochronology. Application in Environmental Sciences*. pp 63–75. Kluwer Acad. Publ., Dordrecht; Boston; London.